

**Satellite- and  
ground-based CO  
total column  
observations**

L. Yurganov et al.

**Satellite- and ground-based CO total  
column observations over 2010 Russian  
fires: accuracy of top-down estimates  
based on thermal IR satellite data.**

**L. Yurganov<sup>1</sup>, V. Rakitin<sup>2</sup>, A. Dzhola<sup>2</sup>, T. August<sup>3</sup>, E. Fokeeva<sup>2</sup>, G. Gorchakov<sup>2</sup>,  
E. Grechko<sup>2</sup>, S. Hannon<sup>1</sup>, A. Karpov<sup>2</sup>, L. Ott<sup>4</sup>, E. Semutnikova<sup>5</sup>, R. Shumsky<sup>2</sup>,  
and L. Strow<sup>1</sup>**

<sup>1</sup>Joint Center for Earth Systems Technology, University of Maryland Baltimore County,  
Baltimore, MD, USA

<sup>2</sup>Obukhov Institute of Atmospheric Physics, Moscow, Russia

<sup>3</sup>EUMETSAT, Darmstadt, Germany

<sup>4</sup>NASA, Goddard Space Flight Center, Greenbelt, MD, USA

<sup>5</sup>Mosecomonitoring, Moscow, Russia

Received: 18 March 2011 – Accepted: 8 April 2011 – Published: 19 April 2011

Correspondence to: L. Yurganov (yurganov@umbc.edu)

Published by Copernicus Publications on behalf of the European Geosciences Union.

[Title Page](#)

[Abstract](#) [Introduction](#)

[Conclusions](#) [References](#)

[Tables](#) [Figures](#)

[⏪](#) [⏩](#)

[◀](#) [▶](#)

[Back](#) [Close](#)

[Full Screen / Esc](#)

[Printer-friendly Version](#)

[Interactive Discussion](#)

## Abstract

Data are presented from three space sounders and two ground-based spectrometers in Moscow and its suburbs during the forest and peat fires that occurred in Central Russia in July–August 2010. The Moscow area was strongly impacted by the CO plume from these fires. Concurrent satellite- and ground-based observations were used to quantify the errors of CO top-down emission estimates. On certain days, CO total columns retrieved from the data of the space-based sounders were 2–3 times less than those obtained from the ground-based sun-tracking spectrometers. The depth of the polluted layer over Moscow was estimated using total column measurements compared with CO volume mixing ratios in the surface layer and on the TV tower and found to be between 180 and 360 m. The missing CO that is the average difference between the CO total column accurately determined by the ground spectrometer and that retrieved by MOPITT and AIRS, was determined for the Moscow area as  $\sim 3 \times 10^{18}$  molec  $\text{cm}^{-2}$ . This value was extrapolated onto the entire plume; subsequently, the CO burden (total mass) over Russia during the fire event was corrected. A top-down estimate of the total emitted CO, obtained by a simple mass balance model increased by 80%–100% due to this correction (up to 40 Tg).

## 1 Introduction

Carbon monoxide (CO) is recognized as a useful tracer of biomass burning and anthropogenic pollution (Logan et al., 1981; Edwards et al., 2004, 2006; McMillan et al., 2010). CO total source is estimated by Holloway et al. (2000) and by Duncan et al. (2007) as  $2360 \pm 100$  Tg  $\text{yr}^{-1}$ . Contributions from wildfires were counted using the GFED3 model by van der Werf et al. (2010), and vary from year to year, both globally and regionally. From 2000 to 2009, global fire emissions varied between 253 (2001) and 388 (2006) Tg  $\text{yr}^{-1}$ , i.e., between 11% and 16% of total source. Uncertainties in these calculations are connected with estimates of burned areas, fuel loads, emission factors, etc. As a way to carry out top-down estimates of CO fire emissions, satellite measurements of CO are of great importance.

12208

ACPD

11, 12207–12250, 2011

## Satellite- and ground-based CO total column observations

L. Yurganov et al.

Title Page

Abstract

Introduction

Conclusions

References

Tables

Figures

⏪

⏩

◀

▶

Back

Close

Full Screen / Esc

Printer-friendly Version

Interactive Discussion



**Satellite- and  
ground-based CO  
total column  
observations**

L. Yurganov et al.

[Title Page](#)[Abstract](#)[Introduction](#)[Conclusions](#)[References](#)[Tables](#)[Figures](#)[Back](#)[Close](#)[Full Screen / Esc](#)[Printer-friendly Version](#)[Interactive Discussion](#)

CO has been measured from space since 1981 (Reichle et al., 1986). Those pioneering observations revealed biomass burning, especially over Africa, as the most prominent global CO feature and confirmed the North-South CO total column (TC) gradient discovered earlier using a ship-based spectrometer (Malkov et al., 1976). CO is now measured operationally by 3 satellite-borne sounders, and the results of most retrievals are available on the Web. CO has very distinct spectral features; the fundamental band and its first overtone, which are located in the Thermal Infrared Red (TIR) and Near Infrared Red (NIR) spectral regions, respectively. Most of the data come from the TIR region (MAPS, MOPITT, AIRS, TES, IASI) near 4.6  $\mu\text{m}$ . For nadir sounding of tropospheric composition, a principal limitation of TIR instruments is their low sensitivity below 2–3 km of altitude, mostly in the boundary layer (BL). As a result, the retrieved CO TC is different from the actual TC; the equation connecting them includes a sensitivity function (averaging kernel), the true profile, and a priori profile; consequently, the real TC cannot be derived from the retrieved one without knowing the true CO profile. However, in absence of strong surface emissions (e.g., wildfires), true CO profiles are close to the a priori profiles and the total error of CO TC retrieval is generally less than  $\pm 10\%$  (Barret et al., 2003; Clerbaux et al., 2008, 2009; Emmons et al., 2004, 2007, 2009; Warner et al., 2007; McMillan et al., 2008, 2010; Yurganov et al., 2008, 2010). This accuracy is high enough for the background CO, because its concentrations in the global unpolluted troposphere vary between 40 ppb in the Southern Hemisphere during the austral summer and 200–300 ppb in the NH during the boreal winter.

MOPITT and AIRS data have been used for quantification of CO sources using top-down inverse global modeling (Pfister et al., 2005; Turquety et al., 2008; Chevallier et al., 2009; Kopacz et al., 2010; Fisher et al., 2010). CO mixing ratios retrieved from AIRS spectra have been used to investigate biomass burning and anthropogenic pollution (McMillan et al., 2005, 2008, 2010; Warner et al., 2007). Unfortunately, inadequate sensitivity to the BL is still a problem for top-down estimates of emission rates, especially for wildfires.

**Satellite- and  
ground-based CO  
total column  
observations**

L. Yurganov et al.

Title Page

Abstract

Introduction

Conclusions

References

Tables

Figures

⏪

⏩

◀

▶

Back

Close

Full Screen / Esc

Printer-friendly Version

Interactive Discussion

In the NIR, the reflected solar radiation prevails over terrestrial emission and the averaging kernel is less dependent on altitude than that for TIR (de Laat et al., 2007, 2010). The first space-based NIR spectrometer SCIAMACHY, sensitive to the 2.3  $\mu\text{m}$  first overtone band of CO, encountered problems connected with the gradual deterioration of spectral channels, low signal to noise ratio, aerosol dependence, etc. (Glaudemans et al., 2008; de Laat et al., 2010); to date, the usefulness of SCIAMACHY data, as well of similar data of NIR channel of MOPITT (Deeter et al., 2009), for scientific needs is limited. In particular, differences between TIR MOPITT V4 and NIR SCIAMACHY (in other words, missing CO) over biomass burning areas never exceeded 0.5 E18 molec  $\text{cm}^{-2}$  (de Laat et al., 2010; Liu et al., 2011) in contradiction to the results of this paper. Moreover, in many cases data of SCIAMACHY over polluted areas were lower than that of MOPITT, a feature explained by cloud effects (Liu et al., 2011).

This paper presents data from three space sounders and two ground-based spectrometers in Moscow and its suburbs during wildfires that occurred in Central Russia in July–August 2010. The Moscow area was strongly impacted by CO plume moved from the peat and forest fires, which occurred to the East and South-East of the city. On certain days the CO TC retrieved from data of space-based sounders was 2–3 times less than those obtained from the ground. With the aid of concurrent measurements of CO volume mixing ratio (VMR) in the surface layer and on the TV tower the depth of polluted layer over Moscow was estimated in the range between 180 and 360 m. The Missing CO (MCO) that is the average difference between the CO TC, determined from the ground and that retrieved by MOPITT and/or AIRS, was determined for the Moscow area as  $\sim 3$  E18 molec  $\text{cm}^{-2}$ ; this value was extrapolated onto the entire plume. CO burden (total mass) during the fire period was added by MCO and used as an input for a simple mass balance model; the influence of this correction on the total emitted CO was estimated between 80% and 100%, depending on the sensor. The total CO emitted by Russian fires was finally estimated between 34 Tg (AIRS) and 40 Tg (MOPITT) with uncertainty  $\sim 30\%$ .

## 2 Instruments, retrieval techniques, validation

### 2.1 Standard satellite data sets

A part of the Terra platform launched in December 1999, the satellite-borne MOPITT instrument is a TIR nadir-viewing gas correlation radiometer described in detail by Drummond (1992). MOPITT uses a cross-track scan with a swath of 700 km, which allows for almost complete coverage of the Earth's surface in about 3 days, with individual pixels of 22 km × 22 km horizontal resolution. The sensitivity of the instrument significantly decreases in the BL (Deeter et al., 2004); therefore, the retrieved TC depends on an a priori profile, especially for highly polluted BL. Version 3 (V3), which is now outdated, used a global uniform a priori. MOPITT V4 data set (Deeter et al., 2010) uses climatologically variable a priori. For both versions, however, huge CO VMR in the BL during wildfires are underestimated.

Yurganov et al. (2010) compared MOPITT V3 with TC measured by 7 ground-based spectrometers and found an instrumental/retrieval drift of 1.4–1.8% per year. This trend was removed in the MOPITT V4 data; a good consistency with aircraft profiles (Emmons et al., 2009) and ground spectrometers (Yurganov et al., 2010) was found; bias in all cases was well inside the limits of ±10%, and no instrumental drift was observed after 2002. MOPITT V4 data can be downloaded from <ftp://l4ftl01.larc.nasa.gov/MOPITT/>.

Launched onboard NASA's Aqua satellite on 4 May 2002, the AIRS cross-track scanning grating spectrometer provides vertical profiles of the atmosphere with a nadir 45 km field-of-regard across a 1650 km swath (Aumann et al., 2003; Chahine et al., 2006). Although primarily designed as a prototype next-generation temperature and water vapor sounder, the broad spectral coverage of AIRS (3.7 to 16 μm with 2378 channels) includes spectral features of O<sub>3</sub>, CO<sub>2</sub>, CH<sub>4</sub>, and CO (Haskins and Kaplan, 1992). With such a broad swath, AIRS infrared spectra and cloud-clearing (Suskind et al., 2003) enable day/night retrievals over nearly 70% of the planet every day (100% daily coverage between 45° and 80° latitude in both hemispheres), with substantial

## Satellite- and ground-based CO total column observations

L. Yurganov et al.

Title Page

Abstract

Introduction

Conclusions

References

Tables

Figures



Back

Close

Full Screen / Esc

Printer-friendly Version

Interactive Discussion



portions of the globe observed twice per day (ascending and descending orbits). Thus, AIRS readily observes global scale transport from large biomass burning sources (McMillan et al., 2005).

AIRS' operational V5 algorithm applies a perturbation function with trapezoidal shapes to retrieve a set of the geophysical states. An eigenvector decomposition technique is employed to a set of modified Jacobian to solve for the geophysical state, and a damping process is used to stabilize the solution (Suskind, et al., 2003). The selection of the number and levels of the trapezoidal functions, the magnitude of the damping constraint, and the choice of the first guess profile all affect the performance of the retrieval (Warner et al., 2007; McMillan et al., 2008). CO retrievals are obtained from the 2160–2200  $\text{cm}^{-1}$  portion of the spectrum on the edge of the fundamental vibration-rotation band of CO (McMillan et al., 2005). A subset of 36 out of 52 spectral channels in the CO region was selected for the operational retrievals using principle component analysis. The parameters used in the retrievals for this study are described by the AIRS Version 5.0 Released Files Description (<http://disc.sci.gsfc.nasa.gov/AIRS/documentation>), also published by McMillan et al. (2011).

The AIRS mixing ratios for the 500 mb level between 15 June and 14 August 2004 were validated by Warner et al. (2006). The satellite data agree with airborne measurements to within an average of 10–15 ppbv. AIRS CO TC was validated by Yurganov et al. (2008, 2010) by the data of NDAC between 2002 and 2007; in the NH AIRS data were generally 3–5% percent underestimated. The largest error, however, was observed in the SH during the austral summer: AIRS overestimates TC by 15–20%. The AIRS retrievals, version 5, are available at (<http://disc.gsfc.nasa.gov/AIRS/index.shtml>).

**Satellite- and ground-based CO total column observations**

L. Yurganov et al.

Title Page

Abstract

Introduction

Conclusions

References

Tables

Figures

⏪

⏩

◀

▶

Back

Close

Full Screen / Esc

Printer-friendly Version

Interactive Discussion



## 2.2 Retrieval algorithms for IASI and ground-based spectrometers; locations of observational sites

IASI is a Fourier Transform Spectrometer deployed at the EUMETSAT platform Metop-A, which measures calibrated spectra of IR radiation emitted from the Earth. IASI has 8461 spectral channels between  $645.00\text{ cm}^{-1}$  and  $2760.00\text{ cm}^{-1}$  ( $15.5\text{ }\mu\text{m}$  and  $3.63\text{ }\mu\text{m}$ ), with a spectral resolution of  $0.5\text{ cm}^{-1}$  after apodisation. The spectral sampling step is  $0.25\text{ cm}^{-1}$ . IASI scans the track inside the range of  $\pm 48.3^\circ$ . The instantaneous field of view has a ground resolution of 12 km at nadir. A more detailed description of the instrument can be found in (Hébert et al., 2004). IASI products are available on-line in the Earth Observation portal: (<http://www.eumetsat.int/Home/Main/DataAccess/EOPortal/index.htm?l=en>)

The retrieval of CO TC for the IASI spectra was performed using two different algorithms. The first one, a spectral fitting algorithm (SFA), uses a radiative transfer model called SARTA, which was originally developed for AIRS as a forward model (Strow et al., 2003), using ECMWF data for temperature, water vapor, and pressure profiles. First, surface skin temperature was adjusted iteratively using 18 IASI window channels between  $957$  and  $964\text{ cm}^{-1}$ . A priori profiles of gases were taken from MOPITT V3 algorithm (CO) and ECMWF ( $\text{H}_2\text{O}$ ). The scaling factors for profiles of gases were retrieved iteratively using 15 (CO) and 9 ( $\text{H}_2\text{O}$ ) channels in the  $2147\text{--}2169\text{ cm}^{-1}$  spectral range. To do this, the partial derivatives of radiance  $\partial R/\partial \text{SF}$  in the IASI channels that correspond to the lines of  $\text{H}_2\text{O}$  and CO were calculated using SARTA, and finally, SF for each iteration and each gas were calculated as  $\text{SF} = (R_{\text{calc}} - R_{\text{obs}})/(\partial R/\partial \text{SF})$ .

This procedure is repeated 4 times. As a result, radiances in the gas-sensitive channels are fitted by the calculated spectrum with some retrieved SF, but radiances between lines (windows) are not due to the aerosol extinction/emission. Aerosol dominates in the windows, but SARTA is designed for the aerosol-free atmosphere. Radiances in the window channels are perturbed by aerosol, and its impact may be as large as a few percent ( $R_{\text{obs}} < R_{\text{calc}}$ ) compared to the aerosol-free case. The SF retrieved for the gases turns out to be overestimated by several percent. To take into account

### Satellite- and ground-based CO total column observations

L. Yurganov et al.

Title Page

Abstract

Introduction

Conclusions

References

Tables

Figures

⏪

⏩

◀

▶

Back

Close

Full Screen / Esc

Printer-friendly Version

Interactive Discussion



**Satellite- and  
ground-based CO  
total column  
observations**

L. Yurganov et al.

Title Page

Abstract

Introduction

Conclusions

References

Tables

Figures

⏪

⏩

◀

▶

Back

Close

Full Screen / Esc

Printer-friendly Version

Interactive Discussion

5 this effect, the calculated radiances for gas-sensitive channels, fitted previously, are divided by  $R_{\text{calc}}(\text{window})/R_{\text{obs}}(\text{window})$ , and the iterative fitting for gas-sensitive channels is performed again. Finally, both lines and windows are fitted, and the aerosol error of the retrieved SF is minimized. Comparisons of CO total columns between IASI and ground-based spectrometer show a good agreement and a low scatter (see below).

10 The second retrieval is based on an artificial neural network (IASI-ANN). This was trained with a collection of synthetic IASI spectra computed with RTIASI-5 for the forward model and a wide range of atmospheric state vectors. The temperature and water vapor profiles were sampled in the ECMWF climatological dataset, while the a priori trace gas profiles were extracted from some runs of the model MOZART. The inputs of this retrieval are a sub-selection of IASI channels, the surface temperature and a coarse temperature profile, the surface pressure and the satellite zenith angle. The theoretical error with the training base is approximately 10%. As a result of global intercomparisons carried out with MOPITT V3 total columns, the typical departures  
15 between the two products were found to be between 10 and 15% (std) and 0 to 15% (bias), varying with the latitude. The global correlation was as high as 0.8 on average. One advantage of such techniques in comparison to line-fitting methods is the relatively much shorter computation time; for example, the processing time for one spectrum is  $\sim 0.1$  ms at an IBM AIX 6.1 computer (4.7 GHz), while the SFA processing of one spectrum at a SunFire x4600, 4x Dual-Core AMD Opteron Processor 8220 (2.8 GHz) takes  
20  $\sim 500$  ms.

25 Two ground sites were equipped with almost identical grating spectrometers. One was deployed on the upper floor of the Institute of Atmospheric Physics (IAP), Russian Academy of Sciences, in downtown Moscow ( $55.74^\circ$  N,  $37.62^\circ$  E, 200 m a.s.l.). Another was at the Zvenigorod Research Station managed by the IAP, located 53 km to the W from the first one ( $55.70^\circ$  N,  $36.78^\circ$  E, 198 m a.s.l.). Sun-tracking Ebert-Fastie grating spectrometers with 855 mm focal length and a grating of  $300$  grooves  $\text{mm}^{-1}$  were employed for measuring absorption spectra of the atmosphere. These instruments, designed and constructed at the IAP (Dianov-Klokov, 1984), have a resolution

of approximately  $0.2\text{ cm}^{-1}$  in the  $2152\text{--}2160\text{ cm}^{-1}$  spectral region, with a signal-to-noise ratio better than 100, and are equipped with a thermoelectrically cooled PbSe detectors. The retrieval SFA code is written in MATLAB by McKernan et al. (1999) and uses standard non-linear least squares procedures provided by MATLAB. Normally, a standard first guess (a priori) profile of CO concentration (the same as that used in MOPITT V3, AIRS V5, and IASI-SFA retrievals: 120 ppb near the surface and decreasing mixing ratio with height down to 80 ppb just below the tropopause) was iteratively scaled to minimize the residual between measured and calculated spectra. Insufficient spectral resolution, precision of spectral calibration, as well as instability in the instrumental function, do not allow for retrieval of CO profiles using this instrument. The CO TC amount is measured with typical estimated uncertainty for an individual measurement of  $\pm 7\text{--}8\%$  (Yurganov et al., 2002). Yurganov et al. (2008) examined a dependency of TC on the a priori CO profile and found a 17% less CO TC for a priori with VMR = 4 ppm near the surface. In other words, a 30-fold change in the BL surface VMR resulted in just a 17% change in the retrieved TC. This low sensitivity to the shape of a priori profile near the surface is a consequence of high sensitivity of the sun-tracking spectrometer to the lower troposphere (see also Sect. 3.2.1 below).

Identical Non-Dispersive IR (NDIR) Thermo Electron 48i-TLE analyzers for local mixing ratio measurements were deployed in Moscow and Zvenigorod. Both have flow rate of  $0.5\text{ L min}^{-1}$ , detection limit 0.04 ppm, 30-s averaging time, linearity  $\pm 1\%$  full scale, response time 60 s, zero noise 0.02 ppm, drift of zero level (24 h):  $<0.1\text{ ppm}$ . Dimensions are  $584 \times 425 \times 219\text{ mm}$ , and weight 25 kg.

One of the Moscow instruments located at the Meteorological Station of the Moscow State University (MSU,  $55.71^\circ\text{ N}$ ,  $37.52^\circ\text{ E}$ , 212 m a.s.l.). CO VMR measurements at the Moscow Ostankino TV tower are performed at three levels above the ground: 2 m, 130 m, and 248 m by the Mosecomonitoring, as a part of the city pollution control network. In Zvenigorod, both the spectrometer and NDIR analyzer are installed side-by-side at the Zvenigorod Research Station. Locations of ground-based instruments are denoted on the map (Fig. 1).

## Satellite- and ground-based CO total column observations

L. Yurganov et al.

Title Page

Abstract

Introduction

Conclusions

References

Tables

Figures

⏪

⏩

◀

▶

Back

Close

Full Screen / Esc

Printer-friendly Version

Interactive Discussion



## 2.3 Vertical sensitivity functions

For MOPITT and AIRS retrieval techniques, CO vertical VMR distribution (profile) is retrieved first, TC is derived as integrated profile. Two averaging kernels characterize these two products: **AKP** for profile and **AKT** for TC. According to Deeter et al. (2004, 2010)

$$\mathbf{x}_{\text{ret}} = \mathbf{x}_a + \mathbf{AKP} * (\mathbf{x} - \mathbf{x}_a) \quad (1)$$

where  $\mathbf{x}_{\text{ret}}$  is a simulation of retrieved profile,  $\mathbf{x}_a$  is an assumed a priori CO profile,  $\mathbf{x}$  is the true profile, matrix **AKP** is the averaging kernel for retrieved profiles, and it is archived together with CO profiles and TC. In Version 4 of MOPITT, **AKP** is determined for the natural logarithm of VMR (see the MOPITT Version 4 Product User's Guide ,<http://www.acd.ucar.edu/mopitt/products.shtml>). **AKT** (vector, in units molec cm<sup>-2</sup>), can be derived from **AKP** using a matrix relation:

$$\mathbf{AKT} = \mathbf{t} * \mathbf{AKP}, \quad (2)$$

where the vector  $\mathbf{t}$  is partial TC in layers for the retrieved profile (molec cm<sup>-2</sup>).

For the atmospheric layers  $\mathbf{t} = 2.12\text{E}13 * (\mathbf{P}_2 - \mathbf{P}_1) * \mathbf{x}_{\text{ret}}$ , where  $\mathbf{P}_2$  and  $\mathbf{P}_1$  are pressures at the bottom and the top of a layer in hPa, respectively. To normalize the vector **AKT**, it is divided by corresponding vector  $\mathbf{t}$ ; the vector **AKTN** is dimensionless.

Retrieval algorithms for ground spectrometers and IASI-SFA provide TC directly by scaling a priori profile. **AKTN** were calculated using a set of TC retrievals from simulated spectra for profiles with known perturbations in layers; a priori in all retrievals was the same (unperturbed). In this case, **AKTN** was calculated using the vector relation:

$$\mathbf{AKTN} = (\mathbf{TC}_{\text{ret}} - \mathbf{TC}_{\text{ret0}}) / (\mathbf{TC}_{\text{true}} - \mathbf{TC}_{\text{true0}}), \quad (3)$$

where  $\mathbf{TC}_{\text{true0}}$  is TC for the standard a priori profile;  $\mathbf{TC}_{\text{true}}$  is TC for the perturbed profile;  $\mathbf{TC}_{\text{ret0}}$  is TC retrieved from simulated spectrum for the standard a priori profile;  $\mathbf{TC}_{\text{ret}}$  is TC retrieved from the perturbed simulated spectrum.

### Satellite- and ground-based CO total column observations

L. Yurganov et al.

Title Page

Abstract

Introduction

Conclusions

References

Tables

Figures

⏪

⏩

◀

▶

Back

Close

Full Screen / Esc

Printer-friendly Version

Interactive Discussion



---

## Satellite- and ground-based CO total column observations

L. Yurganov et al.

---

Title Page

Abstract

Introduction

Conclusions

References

Tables

Figures

⏪

⏩

◀

▶

Back

Close

Full Screen / Esc

Printer-friendly Version

Interactive Discussion



**AKTN** for three space-based and one ground-based instrument are presented in Fig. 2. A striking difference in shapes of the ground- and space-based spectrometers below 500 hPa is explained by the physics of the radiative transfer in the atmosphere. The sensitivity of retrievals from nadir-viewing TIR sounders is determined by the vertical thermal contrast: a zero contrast or, moreover, a thermal inversion should cause zero sensitivity. This situation often realizes in the BL, especially, in winter time, during night time, or in the morning. On the contrary, ground-based spectrometers register high-temperature solar radiation absorbed by the Earth's atmosphere. Line shapes are collision-broadened and are formed by the atmospheric layers with different pressures; central parts of lines are dominated by absorption in the upper troposphere, the wings are formed by the lower altitude layers. Strong lines are saturated in the center (i.e., the radiation is totally absorbed), and **AKTN** (i.e., the sensitivity) is higher in the lower troposphere. For weak lines, which are not saturated in the center, the shape of **AKTN** may be close to constancy with height. In any case (whether the lines are strong or weak), the sensitivity of solar-viewing spectrometers to the BL is much higher than that of space-based spectrometers.

## 2.4 Validation and comparison

For validation, a period between January 2009 and June 2010 was selected as a period with minimal fire activity in Russia (Fig. 3). Each satellite data set was compared to daily mean CO TC measured from the ground. For this analysis, the temporal coincidence criterion was taken the same calendar day (in UTC). Spatial coincidence required a satellite observation in the same  $1^\circ$  latitude  $\times$   $1^\circ$  longitude grid cell as the ground station. The maximum misalignment was 150 km.

In accordance with Yurganov et al. (2008, 2010), the largest discrepancies between ground and space instruments were observed in wintertime (near the seasonal CO maximum) due to two main reasons: first, **AKTN** are lower in wintertime than in summertime in the lower atmosphere (see two cases for IASI, Fig. 2); second, CO profiles are steeper in wintertime due to more stable BL and temperature inversions.



and IASI-ANN in July). AIRS measured lower CO burden during the entire year and during the fire period as well. The black line plotted through the lowest points of AIRS data (Fig. 6) illustrates the way the background CO burden was assumed. This background line was necessary for calculation of pyrogenic CO burden.

## 3.2 Ground-based vs. satellite comparisons

### 3.2.1 VMR in the surface and boundary layers; the depth of polluted layer

Figure 7a and b (note: different y-axis scales) demonstrates a huge increase in CO VMR in the surface layer both in the city and the rural site. Overall means for the pre-fire period were 224 and 351 ppb in the rural and urban sites, respectively. Before the main fires (June–early July, days 150–190), in the rural area low day-to-day variations were superimposed by a distinct diurnal cycle with a nighttime maximum. Weekly variations with maxima on Friday-Saturday were observed in the city. Stable atmospheric conditions and accumulation of CO urban emissions during the week explain this pattern. Starting with 2 August (day 214), Fig. 7b, CO VMR were increasing rapidly and reached maxima of daily means on 7 August (day 219): 9.8 ppm in Moscow, and 8 August (day 220): 7.1 ppm in Zvenigorod. During some days with high pollution, TC measurements were impossible due to strong aerosol dimming that caused instability of sun trackers.

Similar CO VMR were observed in downtown Fairbanks, Alaska (USA) during the 2004 Alaskan wildfire season, which was the worst on record for that area (Wendler et al., 2010). Strong northerly winds advected pollution into Fairbanks from the fire, located to the North of the city. The maximum CO VMR of 10.3 ppm was recorded on 28 June 2004, resulting in an 8-h average VMR of 9.2 ppm. During the day, the 8-hourly averaged CO VMR dropped to 8.6 ppm. Total CO emitted from the fire was estimated as  $30 \pm 5$  Tg CO using inverse modeling and MOPITT v3 data (Pfister et al., 2005).

To determine the depth of the polluted layer we compared satellite and ground TC measurements of CO and in-situ measurements on 9 August in Moscow (day 221). For

## Satellite- and ground-based CO total column observations

L. Yurganov et al.

Title Page

Abstract

Introduction

Conclusions

References

Tables

Figures



Back

Close

Full Screen / Esc

Printer-friendly Version

Interactive Discussion



characterization of CO VMR in the boundary layer, we used TV tower data averaged over the altitudes between 0 and 248 m above the ground. TV tower VMR, surface MSU VMR, and TC of the ground-based Moscow spectrometer are plotted in Fig. 8. Throughout this day, a general decline in CO was observed, both for VMR and TC.

5 The availability of satellite and ground-based measurements gives an opportunity to determine the depth of the polluted layer: (1) MOPITT specifies VMR for the free troposphere above 3 km of altitude for 8 August (the Moscow location was missing in the 9 August MOPITT data set), (2) CO data from TV tower characterize bottom 200 m of the atmosphere, (3) the spectrometer measures CO TC. Spectral fitting and scaling  
10 of a set of 13 a priori profiles were performed for two ground-based spectra at 11:24 and 14:38, Moscow local time (UTC-4 h) (see Fig. 9). The first run (the depth = 0) was carried out with the “background” distribution: 523 ppb from the surface to 700 hPa, and a gradual decline above, according to MOPITT data. For the second run, VMR in the bottom 20 m thick layer of the atmosphere was set equal to the average of CO VMR from TV tower (7 ppm for the AM spectrum and 3.5 ppm for the PM spectrum). For the third run, the depth of polluted air was increased by 20 m with the same VMR, and so on, with the TC in these a priori profiles increasing due to the changing depth of the layer polluted with the same VMR. These profiles were scaled until the calculated CO spectra fit the measured spectra. If the scaling factor is equal to 1 (in other words,  
15 retrieved = a priori), the assumed depth of the polluted layer may be considered close to the real one. The morning retrieval led to the depth of 280 m (the intersection of two blue lines); the afternoon retrieval revealed the depth of 180 m (the intersection of two black lines). Unfortunately, this method is highly uncertain due to the variability of CO VMR in both horizontal and vertical directions. Additional calculations (not plotted on the graph) with AIRS VMR = 322 ppb above the polluted layer resulted in a larger  
20 depth: ~360 m for both cases. However, a useful conclusion can be drawn: the depth of polluted air over Moscow on 9 August 2010 did not exceed a few hundred meters. A similar depth of ~200 m was obtained using the same procedure for Zvenigorod, 4 August 2010.

## Satellite- and ground-based CO total column observations

L. Yurganov et al.

Title Page

Abstract

Introduction

Conclusions

References

Tables

Figures



Back

Close

Full Screen / Esc

Printer-friendly Version

Interactive Discussion



## Satellite- and ground-based CO total column observations

L. Yurganov et al.

Title Page

Abstract

Introduction

Conclusions

References

Tables

Figures

⏪

⏩

◀

▶

Back

Close

Full Screen / Esc

Printer-friendly Version

Interactive Discussion

The algorithm described above is working well for the ground solar-tracking spectrometer but is not working for a TIR nadir-looking spectrometer, which can be illustrated by a failed attempt to do the same with a spectrum of IASI, registered on 9 August, at 11:27, Moscow time, 55.5481° N, 38.5837° E. It was fitted by calculated spectra with the same set of a-priori profiles (red lines in Fig. 9). Calculations were performed using the kCARTA radiative transfer algorithm (DeSouza-Machado et al., 1997). In contrast to the ground spectrometer, we see that the TC retrieved from the IASI spectrum was increasing along with the increasing a priori, a direct consequence of low sensitivity of IASI channels to the concentrations in the BL (see Sect. 2.3 and corresponding figures).

### 3.2.2 Extrapolation of Moscow results onto the entire plume

TC ground measurements in the Moscow area make it possible to estimate the missing CO (MCO), i.e., the difference between TC for two ground-based spectrometers and satellite data. In this section, MCO will be extrapolated onto the entire plume. First, the area of the plume needs to be determined.

AIRS V5 is probably a less accurate CO data set than MOPITT V4, but it ensures 100% daily coverage of the Russian territory, and its data can be used for quantification of the plume area. The latter is determined here as the area with satellite-derived VMR-500 larger than a specified low limit. The low limit of VMR-500 can be determined by comparing periods with and without fires, e.g., 2010 and 2009 over Russia. In 2009, the CO VMR-500 over the entire area of Russia had a narrow and close-to-normal frequency distribution with a maximum near 100 ppb (Fig. 10, blue line); there were just few numbers of measurements above 130 ppb, and practically no data above 150 ppb. Conversely, a 2010 plot (red line) reveals many cases with VMR-500 > 150 ppb.

In this section the Moscow area for the satellite data is chosen as 54.0–57.0° N and 36.0–38.0° E. Daily and spatial averages of VMR-500 are presented for AIRS and MOPITT in Fig. 11a. VMR-500 for both AIRS and MOPITT exceeded 150 ppb in the Moscow/Zvenigorod area between 2 and 9 August 2010 (days 214–221). We consider

150 ppb as the most likely option for the plume boundary; 170 ppb option was used as a less justified case.

Mean values for two ground sites (in E18 molec cm<sup>-2</sup>, number of spectra in parentheses) for 2–9 August are Moscow 7.45 (75); Zvenigorod 5.43 (58); combined 6.31 (133). Zvenigorod displays lower pollution since its location was less impacted by the plume than Moscow. The mean TC measured by satellite sounders in the specified 3° latitude × 2° longitude square (in E18 molec cm<sup>-2</sup>) are MOPITT 3.34; AIRS 3.15. Larger values retrieved from MOPITT data are explained by its slightly higher sensitivity to the BL and, to some extent, a possible bias in the algorithm. Finally, MCO (satellite minus ground) for MOPITT is estimated as 2.97, and for AIRS, 3.16 (all TC values are in 10 E18 molec cm<sup>-2</sup>).

The plume areas for three limits: 130, 150, and 170 ppb, are plotted in Fig. 12a. AIRS grid cells with no data (e.g., cloudy pixels) but located inside the plume were included in the area calculations using a criterium of 2, 3, or 4 adjacent “plume” grids. The area with no data amounts up to 10% of total plume area. Plume periphery has VMR-500 between 130 and 150 ppb (greenish pixels on the map of Fig. 5b).

Primary CO burdens emitted by fires (measured minus background) for four data sets are plotted in Fig. 12b. Also plotted are burdens added by MCO for AIRS and MOPITT in assumption of 150 ppb as a plume boundary.

Accuracy of satellite retrievals for the plume periphery (VMR-500 between 130 and 150 ppb) may be quantified as well. These values of VMR-500 were measured by AIRS over the Moscow area between 23 July and 27 July (days 204–208). During this period, there were measurements in Zvenigorod as well (but, unfortunately, not in Moscow itself). For the Zvenigorod grating, MOPITT, and AIRS, the TC was 2.89, 2.50, and 2.33 E18 molec cm<sup>-2</sup>, respectively. Therefore, MCO for MOPITT and AIRS were 0.39 and 0.56 E18 molec cm<sup>-2</sup>, significantly less than MCO for the “fire week”. Inclusion of the plume periphery changes the corrected burden only by 6.0 and 6.8% for MOPITT and AIRS.

**Satellite- and ground-based CO total column observations**

L. Yurganov et al.

Title Page

Abstract

Introduction

Conclusions

References

Tables

Figures



Back

Close

Full Screen / Esc

Printer-friendly Version

Interactive Discussion



## 4 Mass balance inverse modeling of the Russian fire

### 4.1 Method and testing

Similar to the approach used in the previous papers (Yurganov et al., 2004, 2005, 2008, 2010), the emission of CO is derived from its burden anomaly inside some specified area. This is a simple and fast technique to estimate smoothed daily CO emission rates and total emitted CO. Here, this technique is used primarily as a convenient tool to determine the sensitivity of a top-down estimate to the error of a satellite-borne TIR sounder. Any anomaly is determined as a difference between the measured burden and the “background”, i.e., the burden that would be without fires. The line of background CO burden is plotted through the lowest points of the measured burden in 10-day intervals, and corresponds to the black line in Fig. 6 for the AIRS case, plotted as an example.

The daily anomalies of the CO global emission rate  $P$  ( $\text{Tg CO day}^{-1}$ ) is connected with the daily change in the burden anomaly  $dB/dt$ , daily burden anomaly  $B$ , and time parameters for the sinks TAU: [OH] oxidation  $\text{TAU}_{\text{chem}}$  and wind removal  $\text{TAU}_{\text{trans}}$ :

$$P = dB/dt + B/\text{TAU}_{\text{chem}} + B/\text{TAU}_{\text{trans}} \quad (4)$$

$\text{TAU}_{\text{chem}}$  is calculated from the vertical distributions of monthly mean [OH] tabulated by Spivakovsky et al. (2000). In the mid-latitudes, in contrast to the tropics, blowing out CO prevails over oxidation;  $\text{TAU}_{\text{trans}}$  is estimated using a 3-D chemistry/transport model GEOS-5 driven by assimilated meteorological data from the NASA/GSFC/GEOS/GMAO (Duncan et al., 2007).

The model runs with no biomass burning emissions since 1 July 2010 except for the idealized fire sources of 1.11 Tg per day over a  $3^\circ$  latitude by  $3.75^\circ$  longitude region centered on  $55^\circ$  N,  $45^\circ$  E. The fire sources are tracers of 5-day periods – essentially, the first run represents the fire emissions for 1–5 July, the second represents the fire for 6–10 July, etc. This provides an indication of how long CO mixing ratios remain elevated after burning and how fast it relaxes afterwards (Fig. 13a). In Fig. 13b e-fold

## Satellite- and ground-based CO total column observations

L. Yurganov et al.

Title Page

Abstract

Introduction

Conclusions

References

Tables

Figures

⏪

⏩

◀

▶

Back

Close

Full Screen / Esc

Printer-friendly Version

Interactive Discussion



parameters TAU for time spans with durations between 12–16 days after the fire halts are plotted. The highest TAU (the lowest transport) was observed during the first half of the real fire period; during the second half of the period, the intensity of air circulation was gradually increasing (TAU diminishing).

5 These model simulations give an opportunity to test the performance of the mass balance inverse modeling. All burdens presented in Fig. 13a were taken as “measured” and the emission was retrieved from those. One example of the retrieval (1.11 Tg day<sup>-1</sup> emission was set between days 207 and 211) is plotted in Fig. 14a. The retrieved daily emission in the maximum (1.3 Tg day<sup>-1</sup>) exceeds the input value by 17%, or averaged  
10 over 10 cases, (20 ± 13)%. Small negative values between days 216 and 220 have no physical meaning and are the result of errors in the model; however, this is tolerable for such a simple model. The total emitted CO is overestimated by (30 ± 17)%.

## 4.2 CO emission in 2010

15 First, the CO emitted by Russian fires was estimated using the satellite remote sensing data without any correction (“standard” case). The retrieved CO daily emission rates and components of CO cycle for the MOPITT case are presented in Fig. 14b. The estimates for this case and for other data sets are tabulated in Table 1.

20 MCO, as determined above for the Moscow-Zvenigorod area, are added to the retrieved CO burden for the entire plume. Two cases for the plume boundaries have been used in the calculations, but a value of 150 ppb fits typical Moscow conditions better.

## 5 Discussion

25 The low sensitivity of TIR sensors to the BL prevents an accurate determination of CO emitted by fires. The most reasonable way to resolve this problem is to use satellite spectrometers with NIR spectral range and reflected solar radiation. However, reliable data of this sort are still unavailable. In this situation, preliminary estimates of the error

### Satellite- and ground-based CO total column observations

L. Yurganov et al.

Title Page

Abstract

Introduction

Conclusions

References

Tables

Figures

⏪

⏩

◀

▶

Back

Close

Full Screen / Esc

Printer-friendly Version

Interactive Discussion



Discussion Paper | Discussion Paper | Discussion Paper | Discussion Paper | Discussion Paper

based on a few days with ground-based TC data matching satellite measurements are helpful.

Having Moscow's MCO represent the entire plume is a matter of concern. We consider 150 ppb as a most reasonable boundary for the plume with CO concentrations that are typical for the Moscow area; however, it should be noted that during the entire period of Russian fires (almost a month) the Moscow/Zvenigorod sites were covered by the edge of the main plume only for a week between 2 August and 9 August. Further, during this week, CO VMR-500 over Moscow/Zvenigorod, according to AIRS and MOPITT, was between 150 and 260 ppb. Meanwhile, AIRS CO VMR-500 in the core parts of the plume reached 300 ppb (Figs. 5 and 10). Also, a few days were missing with the highest pollution both in Moscow and Zvenigorod: during these days the solar trackers could not track the Sun properly due to a reduced illumination. The inclusion of these days would most likely increase our estimate of MCO. On the other hand, testing the mass balance algorithm shows 20–30% overestimation (Sect. 4.1). Finally, the accuracy of the given CO total emission (40 Tg) may be estimated as  $\pm 30\%$ .

A good agreement between different satellite sounders and different retrieval techniques for the standard a priori over the strong fires is noteworthy. We consider this a consequence of the same spectral range; higher spectral resolution hardly can help to resolve the problem. The insensitivity to the BL is illustrated by a failed attempt to retrieve the depth of polluted layer using IASI spectra (Fig. 9): the CO channels in calculated spectra are not sensitive to the CO change in the BL; the retrieved amounts are stuck at the first guess.

On the contrary, the ground-based spectrometer allowed estimating the depth of polluted layer if the additional information on the VMR in the BL is available (Fig. 9). Unfortunately, CO variations in the BL both throughout the city and vertically are huge; CO variability above the polluted layer is large as well. Also, CO VMR above the BL retrieved by MOPITT and AIRS are different. Additional calculations with AIRS VMR in the free troposphere resulted in a larger depth than those with MOPITT:  $\sim 360$  m for both cases. Thus, a depth of 200–300 m (for the assumed step-like CO distribution) is

## Satellite- and ground-based CO total column observations

L. Yurganov et al.

Title Page

Abstract

Introduction

Conclusions

References

Tables

Figures



Back

Close

Full Screen / Esc

Printer-friendly Version

Interactive Discussion



just a rough estimate for this. Moreover, we emphasize that this depth is evaluated for Moscow. Much evidence shows that the Moscow area was impacted significantly by low-temperature peat fires with the depth of mixed layer that is usually lower than that for forest fires, especially during the flaming stage (Potter et al., 2002).

5 According to mass balance considerations, correcting the CO burden for the MCO results in doubling emission. We assume that the satellite TIR underestimation of CO TC over the Russian fires can be applied to other wild fire events as well.

Carbon dioxide from wildfires during the last twelve years varied between 5161 (2009) and 9376 Tg CO<sub>2</sub> yr<sup>-1</sup> (1998), according to the inventory by van der Werf  
10 et al. (2010). If the CO bottom-up evaluations of CO emissions are underestimated in the same manner as top-down ones, then CO<sub>2</sub> wildfires emissions could be underestimated as well; they are calculated from similar sources of information.

## 6 Conclusions

- 15 1. The Moscow area was strongly impacted by the plume of wildfires in early August 2010. Two spectrometers deployed in Moscow and in a rural site registered factor of 2 or 3 higher CO TC than CO TC retrieved from data of 3 TIR space-based sounders.
2. Supplemental CO VMR measured in the surface layer and on the TV tower were on an order of magnitude higher than during the preceding period.
- 20 3. A combination of CO VMR with spectroscopically measured CO TC and VMR above 3 km from MOPITT V4 and AIRS V5 revealed the depth of the polluted layer over Moscow as 200–300 m on 9 August 2010.
- 25 4. Data of MOPITT V4 and IASI (2 different retrieval algorithms with a similar a priori) averaged over the Russian territory during August 2010 have been found to be in good agreement during the period of fires: differences did not exceed 3%. TC AIRS V5 data were systematically biased 3–5% downward.

12226

### Satellite- and ground-based CO total column observations

L. Yurganov et al.

Title Page

Abstract

Introduction

Conclusions

References

Tables

Figures



Back

Close

Full Screen / Esc

Printer-friendly Version

Interactive Discussion



5. Averaged underestimation of TC for the Moscow area (missing CO) have been found to be around  $3 \times 10^{18} \text{ molec cm}^{-2}$ ; this value was extrapolated onto the entire plume. Using a simple mass balance model, the total CO emitted by fires was estimated with and without this correction. Taking into account the missing CO increases the retrieved emission 80–100% with a final estimate of total CO emission using MOPITT V4 up to  $(40 \pm 12) \text{ Tg}$ .

## Appendix A

### Acronyms and abbreviations

AIRS: Atmospheric Infrared Sounder

AKP: Averaging Kernel for Profile

AKT: Averaging Kernel for Total column

AKTN: Averaging Kernel for Total column Normalized

ANN: Artificial Neural Network

BL: Boundary Layer

ECMWF: European Center for Medium-Range Weather Forecasts

EUMETSAT: European Organization for the Exploitation of Meteorological Satellites

GEOS: Goddard Earth Observing System model

GMAO: Global Modeling and Assimilation Office

GSFC: Goddard Space Flight Center

IAP: Obukhov Institute of Atmospheric Physics

IASI: Infrared Atmospheric Sounding Interferometer

kCARTA: kCompressed Atmospheric Radiative Transfer Algorithm

MAPS: Measurements of Atmospheric Pollution from Satellite

MCO: Missing CO

MOPITT: Measurements Of Pollution In The Troposphere

MOZART: Model for OZone And Related chemical Tracers

## Satellite- and ground-based CO total column observations

L. Yurganov et al.

Title Page

Abstract

Introduction

Conclusions

References

Tables

Figures

⏪

⏩

◀

▶

Back

Close

Full Screen / Esc

Printer-friendly Version

Interactive Discussion



MSU: Moscow State University  
NDACC: Network for Detection of Atmospheric Composition Change  
NDIR: Non-Dispersive Infrared  
NH: Northern Hemisphere  
5 NIR: Near Infrared  
OMI: Ozone Monitoring Instrument  
RTIASI: Radiative Transfer algorithm for IASI  
SARTA: Stand-Alone Radiative Transfer Algorithm  
SCIAMACHY: SCanning Imaging Absorption SpectroMeter for Atmospheric  
10 ChartographyY  
SF: Scaling Factor  
SFA: Spectral Fitting Algorithm  
SH: Southern Hemisphere  
TC: Total Column  
15 TES: Tropospheric Emission Spectrometer  
TIR: Thermal Infrared  
UTC: Universal Time Coordinated  
VMR: Volume Mixing Ratio  
VMR-500: Volume Mixing Ratio for the 500 hPa atmospheric pressure level

20 *Acknowledgements.* The authors are grateful to Nikolay Elansky (IAP) for the help in using supplemental in situ measurement results. We thank Sergio DeSouza-Machado (UMBC) for the help in a modification of kCARTA model. Merritt Deeter (NCAR, Boulder, USA) clarified issues connected with new versions of MOPITT data. We are grateful to Meinrat Andreae (MPI for Chemistry, Mainz, Germany) for a helpful discussion. This research was supported through  
25 a subcontract with the AIRS Project Office at JPL: “*Optimization, Validation, and Integrated EOS Analysis*”. Measurements in Russia have been possible due to funding from RFBR (grant # 08-05-00659) and ISTC (grant # 3032). We thank the NASA and the EUMETSAT for access to their archived data.

**Satellite- and ground-based CO total column observations**

L. Yurganov et al.

Title Page

Abstract

Introduction

Conclusions

References

Tables

Figures



Back

Close

Full Screen / Esc

Printer-friendly Version

Interactive Discussion



## References

- Aumann, H. H., Chahine, M. T., Gautier, C., Goldberg, M., Kalnay, E., McMillin, L., Revercomb, H., Rosenkranz, P. W., Smith, W. L., Staelin, D. H., Strow, L., and Susskind, J.: AIRS/AMSU/HSB on the Aqua mission: Design, science objectives, data products, and processing systems, *IEEE T. Geosci. Remote*, 41, 253–264, 2003.
- 5 Barret, B., De Mazière, M., and Mahieu, E.: Ground-based FTIR measurements of CO from the Jungfraujoch: characterisation and comparison with in situ surface and MOPITT data, *Atmos. Chem. Phys.*, 3, 2217–2223, doi:10.5194/acp-3-2217-2003, 2003.
- Chahine, M. T., Pagano, T. S., Aumann, H. H., Atlas, R., Barnett, C., Blaisdell, J., Chen, L., Divakarla, M., Fetzer, E. J., Goldberg, M., Gautier, C., Granger, S., Hannon, S., Irion, F. W., Kakar, R., Kalnay, E., Lambrigtsen, B. H., Lee, S.-Y., LeMarshall, J., McMillan, W. W., McMillin, L., Olsen, E. T., Revercomb, H., Rosenkranz, P., Smith, W. L., Staelin, D., Strow, L. L., Susskind, J., Tobin, D., Wolf, W., and Zhou, L.: The Atmospheric Infrared Sounder (AIRS): Providing new insights into weather and climate for the 21st century, *B. Am. Meteorol. Soc.*, 87, 911–926, 2006.
- 15 Chevalier, F.: Sampled Database of 60 Levels Atmospheric Profiles from the ECMWF Analysis, Technical Report, ECMWF EUMETSAT SAF programme Research Report 4; ECMWF, 2001.
- Chevallier, F., Fortems, A., Bousquet, P., Pison, I., Szopa, S., Devaux, M., and Hauglustaine, D. A.: African CO emissions between years 2000 and 2006 as estimated from MOPITT observations, *Biogeosciences*, 6, 103–111, doi:10.5194/bg-6-103-2009, 2009.
- 20 Clerbaux, C., George, M., Turquety, S., Walker, K. A., Barret, B., Bernath, P., Boone, C., Borsdorff, T., Cammas, J. P., Catoire, V., Coffey, M., Coheur, P.-F., Deeter, M., De Mazière, M., Drummond, J., Duchatelet, P., Dupuy, E., de Zafra, R., Eddounia, F., Edwards, D. P., Emmons, L., Funke, B., Gille, J., Griffith, D. W. T., Hannigan, J., Hase, F., Höpfner, M., Jones, N., Kagawa, A., Kasai, Y., Kramer, I., Le Flochmoën, E., Livesey, N. J., López-Puertas, M., Luo, M., Mahieu, E., Murtagh, D., Nédélec, P., Pazmino, A., Pumphrey, H., Ricaud, P., Rinsland, C. P., Robert, C., Schneider, M., Senten, C., Stiller, G., Strandberg, A., Strong, K., Sussmann, R., Thouret, V., Urban, J., and Wiacek, A.: CO measurements from the ACE-FTS satellite instrument: data analysis and validation using ground-based, airborne and spaceborne observations, *Atmos. Chem. Phys.*, 8, 2569–2594, doi:10.5194/acp-8-2569-2008, 2008.
- 30 Clerbaux, C., Boynard, A., Clarisse, L., George, M., Hadji-Lazaro, J., Herbin, H., Hurtmans, D.,

ACPD

11, 12207–12250, 2011

### Satellite- and ground-based CO total column observations

L. Yurganov et al.

Title Page

Abstract

Introduction

Conclusions

References

Tables

Figures

⏪

⏩

◀

▶

Back

Close

Full Screen / Esc

Printer-friendly Version

Interactive Discussion



## Satellite- and ground-based CO total column observations

L. Yurganov et al.

Title Page

Abstract

Introduction

Conclusions

References

Tables

Figures

⏪

⏩

◀

▶

Back

Close

Full Screen / Esc

Printer-friendly Version

Interactive Discussion



Pommier, M., Razavi, A., Turquety, S., Wespes, C., and Coheur, P.-F.: Monitoring of atmospheric composition using the thermal infrared IASI/MetOp sounder, *Atmos. Chem. Phys.*, 9, 6041–6054, doi:10.5194/acp-9-6041-2009, 2009.

Deeter, M. N., Emmons, L. K., Edwards, D. P., Gille, J. C., and Drummond, J. R.: Vertical resolution and information content of CO profiles retrieved by MOPITT, *Geophys. Res. Lett.*, 31, L15112, doi:10.1029/2004GL020235, 2004.

Deeter, M. N., Edwards, D. P., Gille, J. C., and Drummond, J. R.: CO retrievals based on MOPITT near-infrared observations, *J. Geophys. Res.-Atmos.*, 114, D04303, doi:10.1029/2008JD010872, 2009.

Deeter, M. N., Edwards, D. P., Gille, J. C., Emmons, L. K., Francis, G., Ho, S.-P., Mao, D., Masters, D., Worden, H., Drummond, J. R., and Novelli, P. C.: The MOPITT Version 4 CO Product: Algorithm Enhancements, Validation, and Long-Term Stability, *J. Geophys. Res.-Atmos.*, 115, D07306, doi:10.1029/2009JD013005, 2010.

DeSouza-Machado, S., Strow, L., and Hannon, S.: kCompressed atmospheric radiative transfer algorithm (kCARTA), in *Satellite Remote Sensing of Clouds and the Atmosphere, Procs. Of the European Symposium on Aerospace Remote Sensing #3220, Europto Series, Institute of Electrical Engineers, London, Great Britain, 1997.*

Dianov-Klokov, V. I.: Spectroscopic studies of atmospheric pollution over large cities, *Izvestia AN SSSR, Fizika atmosfery i okeana*, 20, 883–900, 1984 (in Russian).

de Laat, A. T. J., Gloudemans, A. M. S., Aben, I., Krol, M., Meirink, J. F., van der Werf, G. R., and Schrijver, H.: Scanning Imaging Absorption Spectrometer for Atmospheric Cartography carbon monoxide total columns: statistical evaluation and comparison with chemistry transport model results, *J. Geophys. Res.-Atmos.*, 112, D21306, doi:10.1029/2007jd009378, 2007.

de Laat, A. T. J., Gloudemans, A. M. S., Aben, I., and Schrijver, H.: Global evaluation of SCIAMACHY and MOPITT carbon monoxide column differences for 2004–2005, *J. Geophys. Res.-Atmos.*, 115, D06307, doi:10.1029/2009jd012698, 2010.

Duncan, B. N., Logan, J. A., Bey, I., Megretskaia, I. A., Yantosca, R. M., Novelli, P. C., Jones, N. B., and Rinsland, C. P.: Global budget of CO, 1988–1997: Source estimates and validation with a global model, *J. Geophys. Res.-Atmos.*, 112, D22301, doi:10.1029/2007JD008459, 2007.

Drummond, J. R. : Measurements of Pollution in the Troposphere (MOPITT), in: *The Use of EOS for Studies of Atmospheric Physics*, edited by Gille, J. C. and Visconti, G., 77–101,

## Satellite- and ground-based CO total column observations

L. Yurganov et al.

Title Page

Abstract

Introduction

Conclusions

References

Tables

Figures

⏪

⏩

◀

▶

Back

Close

Full Screen / Esc

Printer-friendly Version

Interactive Discussion

North-Holland, NY, 1992.

Edwards, D. P., Emmons, L. K., Hauglustaine, D. A., Chu, A., Gille, J. C., Kaufman, Y. J., Pétron, G., Yurganov, L. N., Giglio, L., Deeter, M. N., Yudin, V., Ziskin, D. C., Warner, J., Lamarque, J.-F., Francis, G. L., Ho, S. P., Mao, D., Chan, J., and Drummond, J. R.: Observations of Carbon Monoxide and Aerosol From the Terra Satellite: Northern Hemisphere Variability, *J. Geophys. Res.-Atmos.*, 109, D24202, doi:10.1029/2004JD004727, 2004.

Edwards, D. P., Emmons, L. K., Gille, J. C., Chu, A., Atti'e, J.-L., Giglio, L., Wood, S. W., Haywood, J., Deeter, M. N., Massie, S. T., Ziskin, D. C., and Drummond J. R.: Satellite-observed pollution from Southern Hemisphere biomass burning, *J. Geophys. Res.-Atmos.*, 111, D14312, doi:10.1029/2005JD006655, 2006.

Emmons, L. K., Deeter, M. N., Gille, J. C., Edwards, D. P., Atti'e, J.-L., Warner, J., Ziskin, D., Francis, G., Khattatov, B., Yudin, V., Lamarque, J.-F., Ho, S.-P., Mao, D., Chen, J. S., Drummond, J., Novelli, P., Sachse, G., Coffey, M. T., Hannigan, J. W., Gerbig, C., Kawakami, S., Kondo, Y., Takegawa, N., Schlager, H., Baehr, J., and Ziereis, H.: Validation of Measurements of Pollution in the Troposphere (MOPITT) CO retrievals with aircraft in situ profiles, *J. Geophys. Res.-Atmos.*, 109, D03309, doi:10.1029/2003JD004101, 2004.

Emmons, L. K., Pfister, G. G., Edwards, D. P., Gille, J. C., Sachse, G., Blake, D., Wofsy S., Gerbig, C., Matross, D., and Nédélec, P.: Measurements of Pollution in the Troposphere (MOPITT): validation exercises during summer 2004 field campaigns over North America, *J. Geophys. Res.-Atmos.*, 112, D12S02, doi:10.1029/2006JD007833, 2007.

Emmons, L. K., Edwards, D. P., Deeter, M. N., Gille, J. C., Campos, T., Nédélec, P., Novelli, P., and Sachse, G.: Measurements of Pollution In The Troposphere (MOPITT) validation through 2006, *Atmos. Chem. Phys.*, 9, 1795–1803, doi:10.5194/acp-9-1795-2009, 2009.

Fisher, J. A., Jacob, D. J., Purdy, M. T., Kopacz, M., Le Sager, P., Carouge, C., Holmes, C. D., Yantosca, R. M., Batchelor, R. L., Strong, K., Diskin, G. S., Fuelberg, H. E., Holloway, J. S., Hyer, E. J., McMillan, W. W., Warner, J., Streets, D. G., Zhang, Q., Wang, Y., and Wu, S.: Source attribution and interannual variability of Arctic pollution in spring constrained by aircraft (ARCTAS, ARCPAC) and satellite (AIRS) observations of carbon monoxide, *Atmos. Chem. Phys.*, 10, 977–996, doi:10.5194/acp-10-977-2010, 2010.

Gloudemans, A. M. S., Schrijver, H., Hasekamp, O. P., and Aben, I.: Error analysis for CO and CH<sub>4</sub> total column retrievals from SCIAMACHY 2.3 μm spectra, *Atmos. Chem. Phys.*, 8, 3999–4017, doi:10.5194/acp-8-3999-2008, 2008.

Haskins, R. and Kaplan, L.: Remote sensing of trace gases using the Atmospheric InfraRed

## Satellite- and ground-based CO total column observations

L. Yurganov et al.

Title Page

Abstract

Introduction

Conclusions

References

Tables

Figures

⏪

⏩

◀

▶

Back

Close

Full Screen / Esc

Printer-friendly Version

Interactive Discussion

Sounder, in: IRS'92: Current Problems in Atmospheric Radiation: Proceedings of the International Radiation Symposium, Tallinn, Estonia, 3–8 August 1992, edited by: Keevallik, S. and Karner, O., 278–281, A. Deepak, Hampton, Va., 1992.

Hébert, Ph., Blumstein, D., Buil, C., Carlier, T., Chalon, G., Astruc, P., Clauss, A., Siméoni, D., and Tournier, B.: IASI instrument: technical description and measured performances, in: Proceedings of the 5th International Conference on Space Optics (ICSO 2004), 30 March–2 April 2004, Toulouse, France, edited by: Warmbein, B., ESA SP-554, Noordwijk, Netherlands: ESA Publications Division, ISBN 92-9092-865-4, 49–56, 2004.

Kopacz, M., Jacob, D. J., Fisher, J. A., Logan, J. A., Zhang, L., Megretskaia, I. A., Yantosca, R. M., Singh, K., Henze, D. K., Burrows, J. P., Buchwitz, M., Khlystova, I., McMillan, W. W., Gille, J. C., Edwards, D. P., Eldering, A., Thouret, V., and Nedelec, P.: Global estimates of CO sources with high resolution by adjoint inversion of multiple satellite datasets (MOPITT, AIRS, SCIAMACHY, TES), *Atmos. Chem. Phys.*, 10, 855–876, doi:10.5194/acp-10-855-2010, 2010.

Liu, C., Beirle, S., Butler, T., Liu, J., Hoor, P., Jöckel, P., Penning de Vries, M., Pozzer, A., Frankenberg, C., Lawrence, M. G., Lelieveld, J., Platt, U., and Wagner, T.: Application of SCIAMACHY and MOPITT CO total column measurements to evaluate model results over biomass burning regions and Eastern China, *Atmos. Chem. Phys. Discuss.*, 11, 1265–1331, doi:10.5194/acpd-11-1265-2011, 2011.

Logan, J. A., Prather, M. J., Wofsy, S. C., and McElroy, M. B.: Tropospheric chemistry: A global perspective, *J. Geophys. Res.-Atmos.*, 86, 7210–7354, 1981.

Malkov, I. P., Yurganov, L. N., and Dianov-Klokov, V. I.: Measurements of CO and CH<sub>4</sub> contents in the Northern and Southern hemispheres (preliminary results), *Izv. Acad. Sci. USSR, Atmos. Oceanic Phys., Engl. Transl.*, 12, 754–757, 1976.

McKernan, E., Yurganov, L. N., Tolton, B. T., and Drummond, J. R.: MOPITT validation using ground-based IR spectroscopy, *Proc. SPIE*, 3756, 486–491, 1999.

McMillan, W. W., Barnet, C., Strow, L., Chahine, M. T., McCourt, M. L., Warner, J. X., Novelli, P. C., Korontzi, S., Maddy, E. S., and Datta, S.: Daily global maps of carbon monoxide from NASA's Atmospheric Infrared Sounder, *Geophys. Res. Lett.*, 32, L11801, doi:10.1029/2004GL021821, 2005.

McMillan, W. W., Warner, J. X., McCourt-Comer, M., Maddy, E., Chu, A., Sparling, L., Eloranta, E., Hoff, R., Sachse, G., Barnet, C., Razenkov, I., and Wolf, W.: AIRS views transport from 12 to 22 July 2004 Alaskan/Canadian fires: Correlation of AIRS CO and MODIS AOD with for-

## Satellite- and ground-based CO total column observations

L. Yurganov et al.

Title Page

Abstract

Introduction

Conclusions

References

Tables

Figures

⏪

⏩

◀

▶

Back

Close

Full Screen / Esc

Printer-friendly Version

Interactive Discussion



ward trajectories and comparison of AIRS CO retrievals with DC-8 in situ measurements during INTEX-A/ICARTT, *J. Geophys. Res.-Atmos.*, 113, D20301, doi:10.1029/2007JD009711, 2008.

McMillan, W. W., Pierce, R., Sparling, L. C., Osterman, G., McCann, K., Fischer, M. L., Rappenglueck, B., Newton, R., Turner, D. D., Kittaka, C., Evans, K., Biraud, S., Lefer, B., Andrews, A., and Oltmans, S.: An Observational and modeling strategy to investigate the impact of remote sources on local air quality: A Houston, Texas case study from TEXAQS II, *J. Geophys. Res.-Atmos.*, 115, D01301, doi:10.1029/2009JD011973, 2010.

McMillan, W. W., Evans, K., Barnett, C., Maddy, E., Sachse, G., and Diskin, G.: Validating the AIRS Version 5 CO Retrieval with DACOM in situ Measurements During INTEX-A and -B, *IEEE T. Geosci. Remote*, 99, 1–12, ISSN: 0196-2892, doi:10.1109/TGRS.2011.2106505, 2011.

Pfister, G., Hess, P. G., Emmons, L. K., Lamarque, J.-F., Wiedmeyer, C., Edwards, C. P., Petron, G., Gille, J. C., and Sachse, G. W.: Quantifying CO emissions from the 2004 Alaskan wildfires using MOPITT-CO data, *Geophys. Res. Lett.*, 32, L11809, doi:10.1029/2005GL022995, 2005.

Potter, B. E.: A dynamics based view of atmosphere-fire interactions, *Int. J. Wildland Fire*, 11, 247–255, 2002.

Reichle, H. G., Connors, V. S., Holland, J. A., Hypes, W. D., Wallio, H. A., Casas, J. C., Gormsen, B. B., Saylor, M. S., and Hesketh, W. D.: Middle and upper tropospheric carbon monoxide mixing ratios as measured by a satellite-borne remote sensor during November 1981, *J. Geophys. Res.-Atmos.*, 91, 10865–10887, 1986.

Spivakovsky, C. M., Logan, J. A., Montzka, S. A., Balkanski, Y. J., Foreman-Fowler, M., Jones, D., Horowitz, L., Fusco, A., Brenninkmeijer, C. A. M., Prather, M. J., Wofsy, S. C., and McElroy, M. B.: Three-dimensional climatological distribution of tropospheric OH: Update and evaluation, *J. Geophys. Res.*, 105, 8931–8980, 2000.

Strow, L. L., Hannon, S. E., de Souza-Machado, S., Motteler, H. E., and Tobin, D.: An overview of the AIRS radiative transfer model, *IEEE T. Geosci. Remote*, 41, 303–313, doi:10.1109/TGRS.2002.808244, 2003.

Susskind, J., Barnett, C. D., and Blaisdell, J. M.: Retrieval of atmospheric and surface parameters from AIRS/AMSU/HSB data in the presence of clouds, *IEEE T. Geosci. Remote*, 41, 390–409, 2003.

Torres, O., Bhartia, P. K., Herman, J. R., and Ahmad, Z.: Derivation of aerosol properties from

## Satellite- and ground-based CO total column observations

L. Yurganov et al.

Title Page

Abstract

Introduction

Conclusions

References

Tables

Figures

⏪

⏩

◀

▶

Back

Close

Full Screen / Esc

Printer-friendly Version

Interactive Discussion

satellite measurements of backscattered ultraviolet radiation. *Theoretical Basis*, *J. Geophys. Res.-Atmos.*, 103, 17099–17110, 1998.

Turquety, S., Clerbaux, C., Law, K., Coheur, P.-F., Cozic, A., Szopa, S., Hauglustaine, D. A., Hadji-Lazaro, J., Gloudemans, A. M. S., Schrijver, H., Boone, C. D., Bernath, P. F., and Edwards, D. P.: CO emission and export from Asia: an analysis combining complementary satellite measurements (MOPITT, SCIAMACHY and ACE-FTS) with global modeling, *Atmos. Chem. Phys.*, 8, 5187–5204, doi:10.5194/acp-8-5187-2008, 2008.

van der Werf, G. R., Randerson, J. T., Giglio, L., Collatz, G. J., Mu, M., Kasibhatla, P. S., Morton, D. C., DeFries, R. S., Jin, Y., and van Leeuwen, T. T.: Global fire emissions and the contribution of deforestation, savanna, forest, agricultural, and peat fires (1997–2009), *Atmos. Chem. Phys.*, 10, 11707–11735, doi:10.5194/acp-10-11707-2010, 2010.

Warner, J. M. M. C., Barnet, C. D., McMillan, W. W., Wolf, W., Maddy, E., and Sachse, G.: comparison of satellite tropospheric carbon monoxide measurements from AIRS and MOPITT during INTEX-A, *J. Geophys. Res.-Atmos.*, 112, D12S17, doi:10.1029/2006JD007925, 2007.

Wendler, G., Conner, J., Moore, B., Shulski, M., and Stuefer, M.: Climatology of Alaskan wildfires with special emphasis on the extreme year of 2004, *Theor. Appl. Climatol.*, doi:10.1007/s00704-010-0357-9, (<http://www.springerlink.com/content/j8h8j54t480k3522/fulltext.pdf>), 2010.

Yurganov, L. N., Grechko, E. I., and Dzhola, A. V.: Long-term measurements of carbon monoxide over Russia using a spectrometer of medium resolution, *Recent Res. Devel. Geophys.*, 4, 249–265, 2002.

Yurganov, L. N., Blumenstock, T., Grechko, E. I., Hase, F., Hyer, E. J., Kasischke, E. S., Koike, M., Kondo, Y., Kramer, I., Leung, F.-Y., Mahieu, E., Mellqvist, J., Notholt, J., Novelli, P. C., Rinsland, C. P., Scheel, H.-E., Schulz, A., Strandberg, A., Sussmann, R., Tanimoto, H., Velazco, V., Zander, R., and Zhao, Y.: A quantitative assessment of the 1998 carbon monoxide emission anomaly in the northern hemisphere based on total column and surface concentration measurements, *J. Geophys. Res.*, 109, D15305, doi:10.1029/2004JD004559, 2004.

Yurganov, L. N., Duchatelet, P., Dzhola, A. V., Edwards, D. P., Hase, F., Kramer, I., Mahieu, E., Mellqvist, J., Notholt, J., Novelli, P. C., Rockmann, A., Scheel, H. E., Schneider, M., Schulz, A., Strandberg, A., Sussmann, R., Tanimoto, H., Velazco, V., Drummond, J. R., and Gille, J. C.: Increased Northern Hemispheric carbon monoxide burden in the troposphere in 2002 and 2003 detected from the ground and from space, *Atmos. Chem. Phys.*, 5, 563–573,

doi:10.5194/acp-5-563-2005, 2005.

Yurganov, L., McMillan, W., Dzhola, A., Grechko, E., Jones, N., and van der Werf, G.: Global AIRS and MOPITT CO Measurements: Validation, Comparison, and Links to Biomass Burning Variations and Carbon Cycle, J. Geophys. Res.-Atmos., 113, D09301, doi:10.1029/2007JD009229, 2008.

5 Yurganov, L., McMillan, W., Grechko, E., and Dzhola, A.: Analysis of global and regional CO burdens measured from space between 2000 and 2009 and validated by ground-based solar tracking spectrometers, Atmos. Chem. Phys., 10, 3479–3494, doi:10.5194/acp-10-3479-2010, 2010.

ACPD

11, 12207–12250, 2011

## Satellite- and ground-based CO total column observations

L. Yurganov et al.

Title Page

Abstract

Introduction

Conclusions

References

Tables

Figures

⏪

⏩

◀

▶

Back

Close

Full Screen / Esc

Printer-friendly Version

Interactive Discussion



## Satellite- and ground-based CO total column observations

L. Yurganov et al.

Title Page

Abstract

Introduction

Conclusions

References

Tables

Figures

⏪

⏩

◀

▶

Back

Close

Full Screen / Esc

Printer-friendly Version

Interactive Discussion



**Table 1.** CO emission rates derived from the data of space sounders using mass balance inverse modeling for standard a priori and for the burdens corrected for MCO. Corrections were applied to the satellite data inside the plume; the boundaries of the plume were specified by 150 ppb (main case) and 170 ppb (supplementary case). In parentheses are the given ratios of emission estimates to the standard values (first two lines in the table). For comparisons to other techniques, the emissions may be diminished by 20–30% because of an error introduced by the model (Sect. 4.1). MCO are added to the retrieved CO if we assume Moscow-Zvenigorod area to be representative of the entire plume.

Data set and boundary VMR-500 for the plume	Total CO emitted between 15 July and 31 August, Tg	Maximum daily emission rate, Tg day <sup>-1</sup>
MOPITT V4, standard	22.3	1.25
AIRS V5, standard	16.8	1.07
IASI SFA, standard	24.8	1.8
IASI ANN, standard	18.1	1.09
MOPITT, 150 ppb	39.6 (1.78)	2.24 (1.79)
MOPITT, 170 ppb	32.4(1.45)	1.94 (1.55)
AIRS, 150 ppb	33.7(2.00)	2.20 (2.05)
AIRS, 170 ppb	26.3 (1.56)	1.91 (1.78)

## Satellite- and ground-based CO total column observations

L. Yurganov et al.



**Fig. 1.** Moscow, Russia, locations of ground-based instruments.

Title Page

Abstract

Introduction

Conclusions

References

Tables

Figures

⏪

⏩

◀

▶

Back

Close

Full Screen / Esc

Printer-friendly Version

Interactive Discussion

## Satellite- and ground-based CO total column observations

L. Yurganov et al.

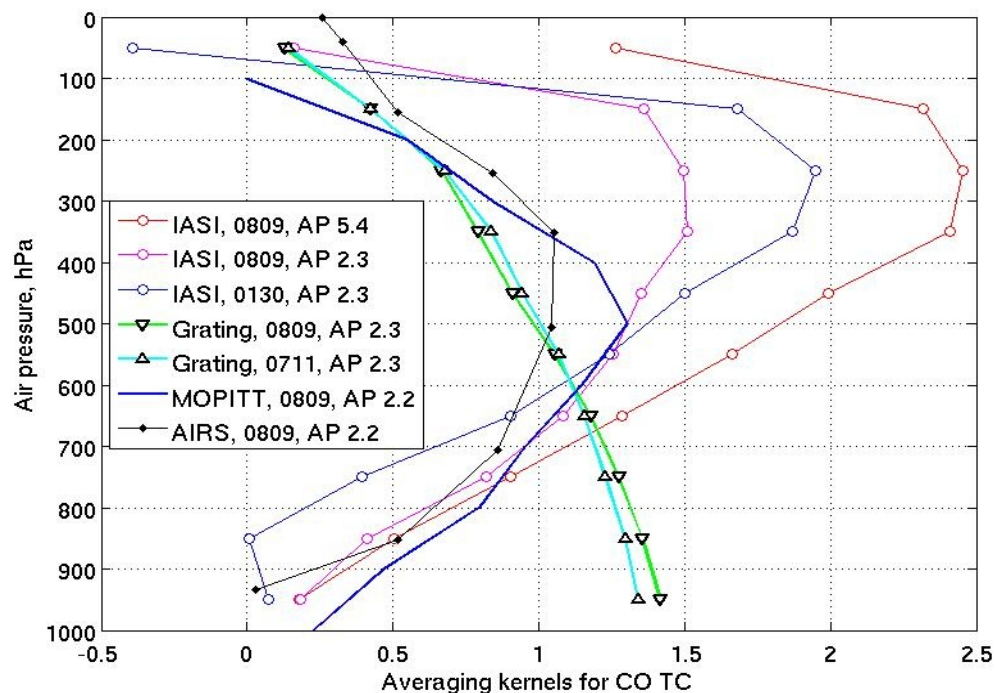


**Fig. 2.** Normalized averaging kernels for CO TC retrieved from data of space- and ground-based instruments, various days of 2010 (e.g., 0809 corresponds to 9 August 2010). A priori profiles: AP 5.4 corresponds to: CO TC equal to  $5.4 \text{ E}18 \text{ molec cm}^{-2}$ , etc.

Title Page

Abstract

Introduction

Conclusions

References

Tables

Figures

◀

▶

◀

▶

Back

Close

Full Screen / Esc

Printer-friendly Version

Interactive Discussion

**Satellite- and  
ground-based CO  
total column  
observations**

L. Yurganov et al.

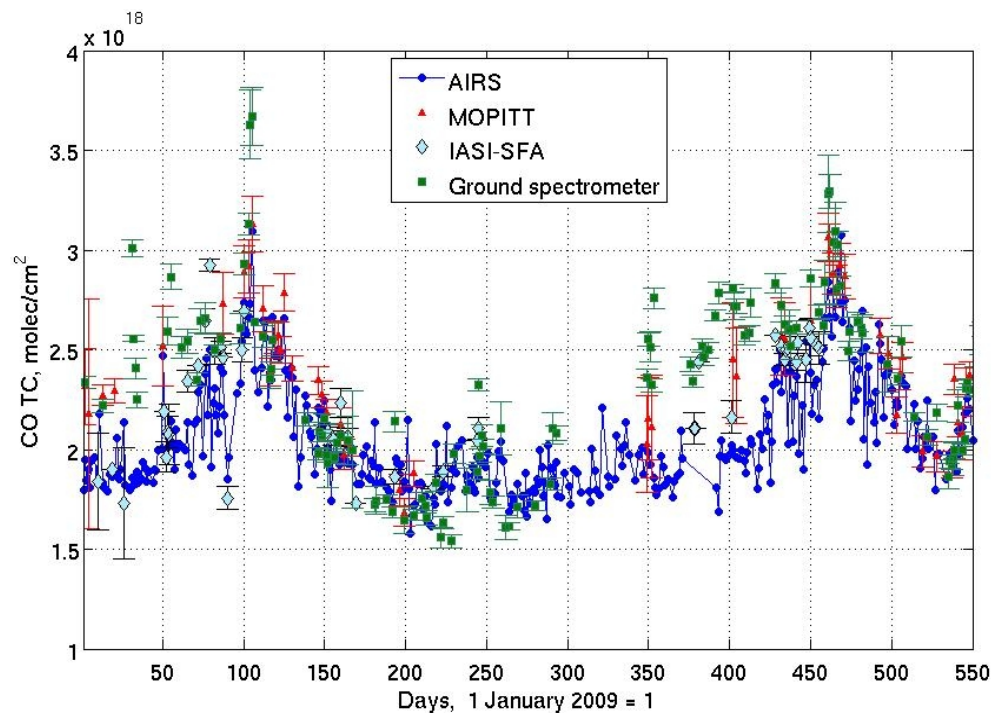


**Fig. 3.** Daily mean CO TC retrieved from spectra recorded by 3 sounders and Zvenigorod ground-based spectrometer. Vertical bars are standard deviations of individual measurements.

[Title Page](#)[Abstract](#)[Introduction](#)[Conclusions](#)[References](#)[Tables](#)[Figures](#)[◀](#)[▶](#)[◀](#)[▶](#)[Back](#)[Close](#)[Full Screen / Esc](#)[Printer-friendly Version](#)[Interactive Discussion](#)

## Satellite- and ground-based CO total column observations

L. Yurganov et al.

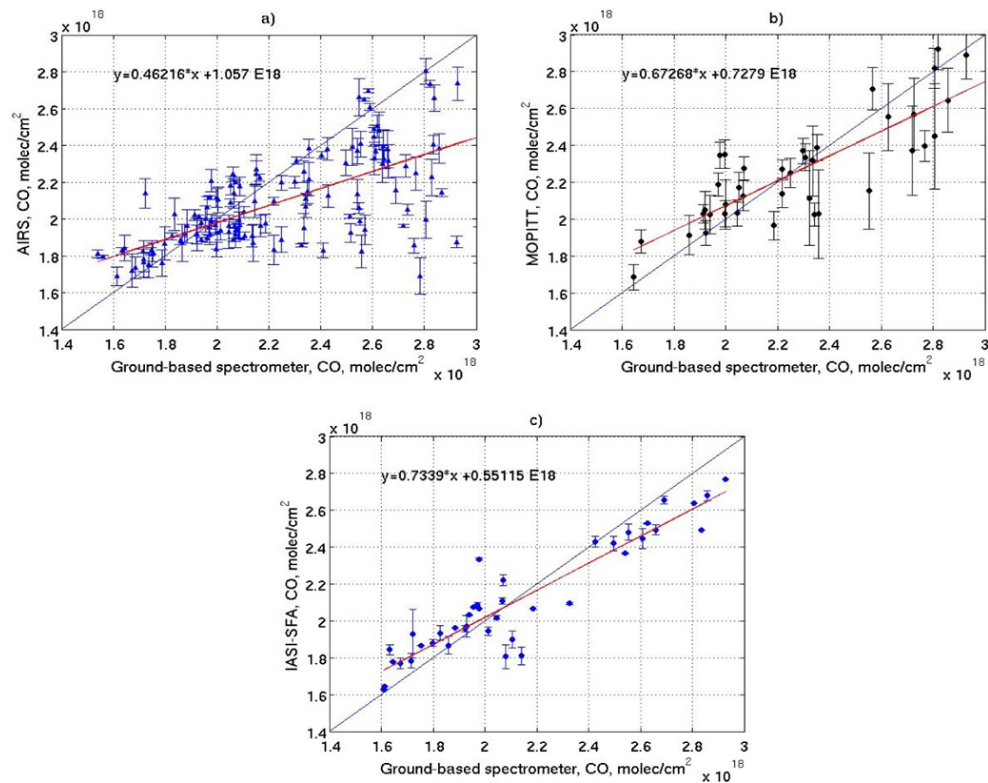


**Fig. 4.** Scattergrams of CO TC for 3 sounders compared to ground data over Zvenigorod for matching days between January 2009 and June 2010. **(a)** AIRS; **(b)** MOPITT; **(c)** IASI-SFA.

Title Page

Abstract

Introduction

Conclusions

References

Tables

Figures

◀

▶

◀

▶

Back

Close

Full Screen / Esc

Printer-friendly Version

Interactive Discussion

**Satellite- and ground-based CO total column observations**

L. Yurganov et al.

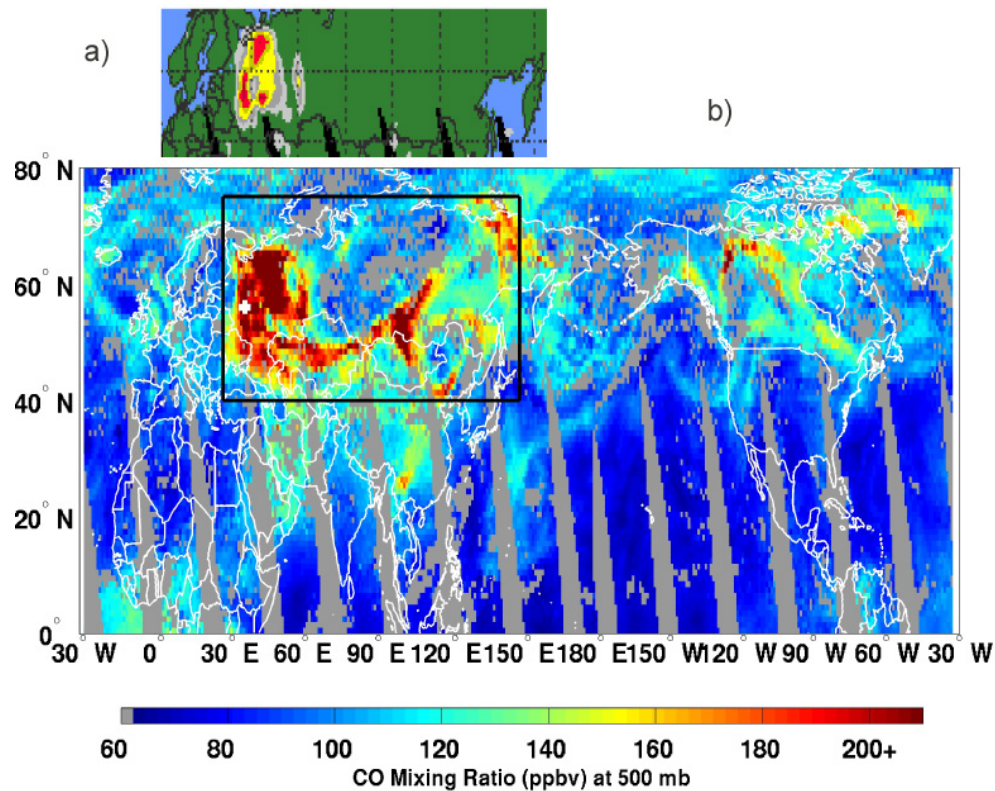


**Fig. 5.** (a) Map of OMI aerosol index for 9 August 2010. (b) Distribution of CO VMR-500 for 9 August 2010, according to AIRS. Black square is the area: 40° N–75° N, 30° E–150° E. Location of Moscow is marked by a white cross.

## Satellite- and ground-based CO total column observations

L. Yurganov et al.

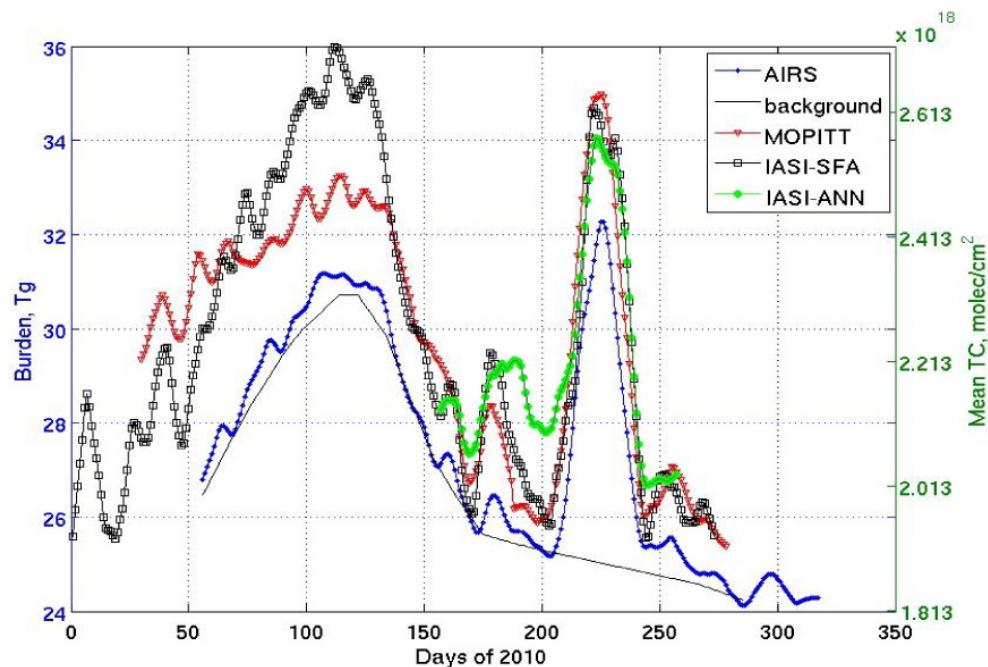


**Fig. 6.** Averaged over the area  $40^{\circ}$ – $75^{\circ}$  N,  $30^{\circ}$ – $150^{\circ}$  E and smoothed CO TC values (right scale) and corresponding burdens (left scale) according to standard data of MOPITT V4 and AIRS V5, as well as IASI, in 2010. For retrieval algorithms IASI-SFA and IASI-ANN see text. Background line is plotted through the lowest points of data before smoothing in 10-days intervals; AIRS background is shown as an example.

[Title Page](#)[Abstract](#)[Introduction](#)[Conclusions](#)[References](#)[Tables](#)[Figures](#)[◀](#)[▶](#)[◀](#)[▶](#)[Back](#)[Close](#)[Full Screen / Esc](#)[Printer-friendly Version](#)[Interactive Discussion](#)

**Satellite- and  
ground-based CO  
total column  
observations**

L. Yurganov et al.

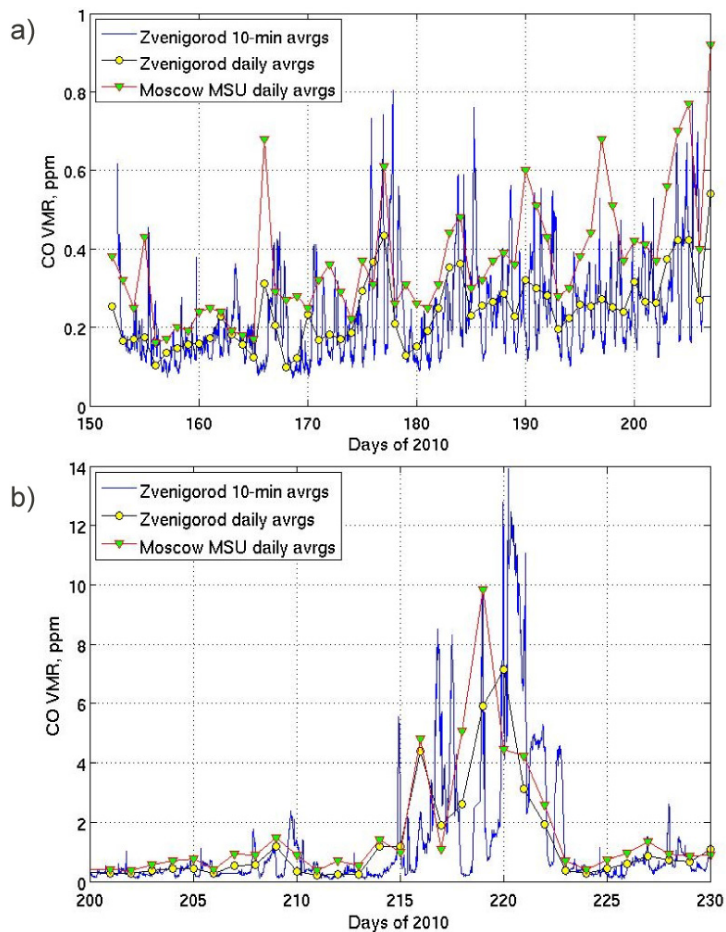


**Fig. 7.** CO VMR in the surface layer in Moscow and rural site Zvenigorod: **(a)** before, and **(b)** during the fire period. Ticks correspond to 12:00 Moscow local time (UTC–4 h).

[Title Page](#)[Abstract](#)[Introduction](#)[Conclusions](#)[References](#)[Tables](#)[Figures](#)[◀](#)[▶](#)[◀](#)[▶](#)[Back](#)[Close](#)[Full Screen / Esc](#)[Printer-friendly Version](#)[Interactive Discussion](#)

## Satellite- and ground-based CO total column observations

L. Yurganov et al.

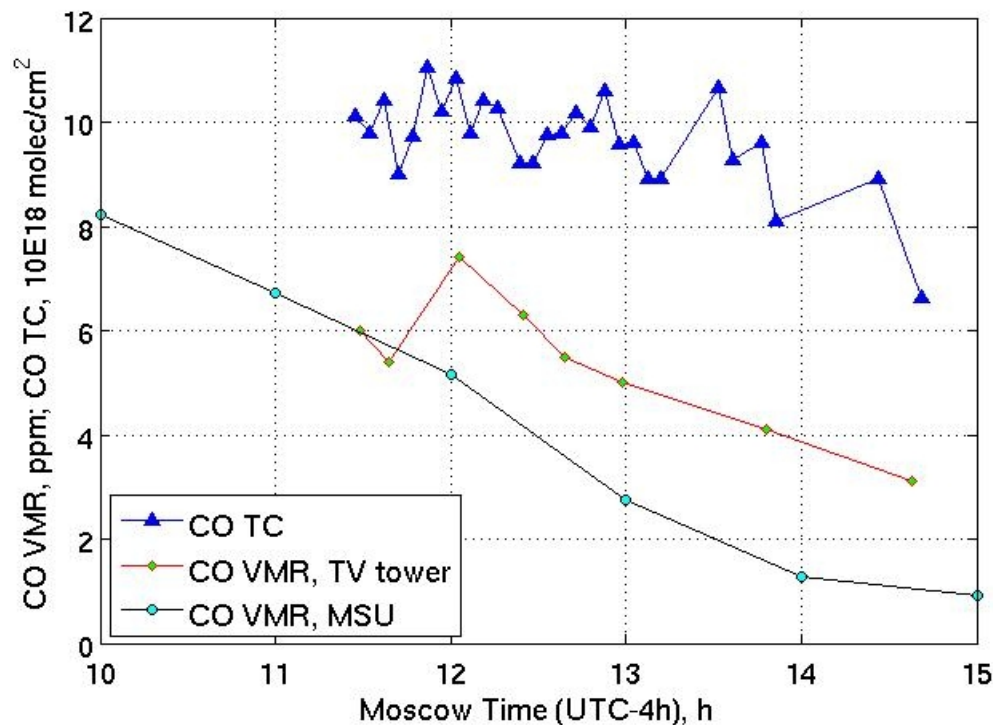


**Fig. 8.** Moscow, 9 August 2010. CO TC retrieved from spectra of ground spectrometer are plotted in units  $E18 \text{ molec cm}^{-2}$ . Also, CO VMR in ppm in the surface layer, MSU, and the data for the TV tower averaged over the altitudes 0–248 m above the surface. For site locations see Fig. 1.

[Title Page](#)[Abstract](#)[Introduction](#)[Conclusions](#)[References](#)[Tables](#)[Figures](#)[◀](#)[▶](#)[◀](#)[▶](#)[Back](#)[Close](#)[Full Screen / Esc](#)[Printer-friendly Version](#)[Interactive Discussion](#)

## Satellite- and ground-based CO total column observations

L. Yurganov et al.

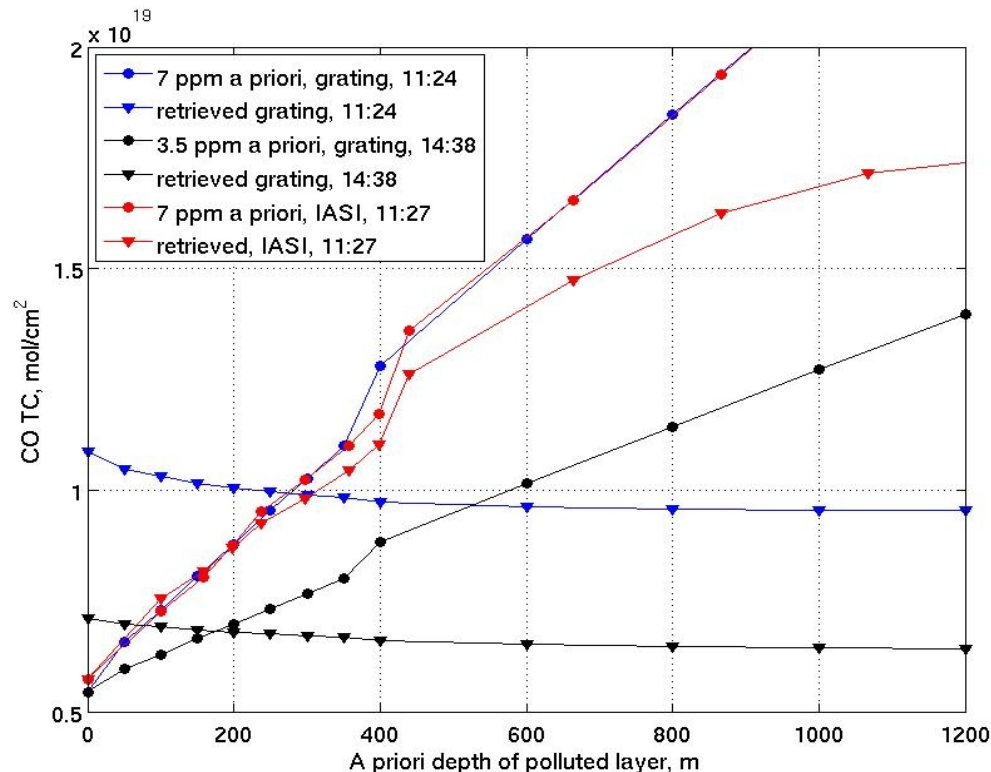


**Fig. 9.** Moscow, 9 August 2010. Ground-based grating total columns for CO a priori profiles (circles) and retrieved TC (triangles) before noon and after noon. A priori profiles differ by the depth of polluted air with VMR 7 and 3.5 ppm. Intersections of lines of the same color (blue and black) correspond to the most probable depths of polluted air and retrieved TC. IASI (red) does not ensure a definite solution.

**Satellite- and ground-based CO total column observations**

L. Yurganov et al.

Title Page

Abstract

Introduction

Conclusions

References

Tables

Figures

◀

▶

◀

▶

Back

Close

Full Screen / Esc

Printer-friendly Version

Interactive Discussion

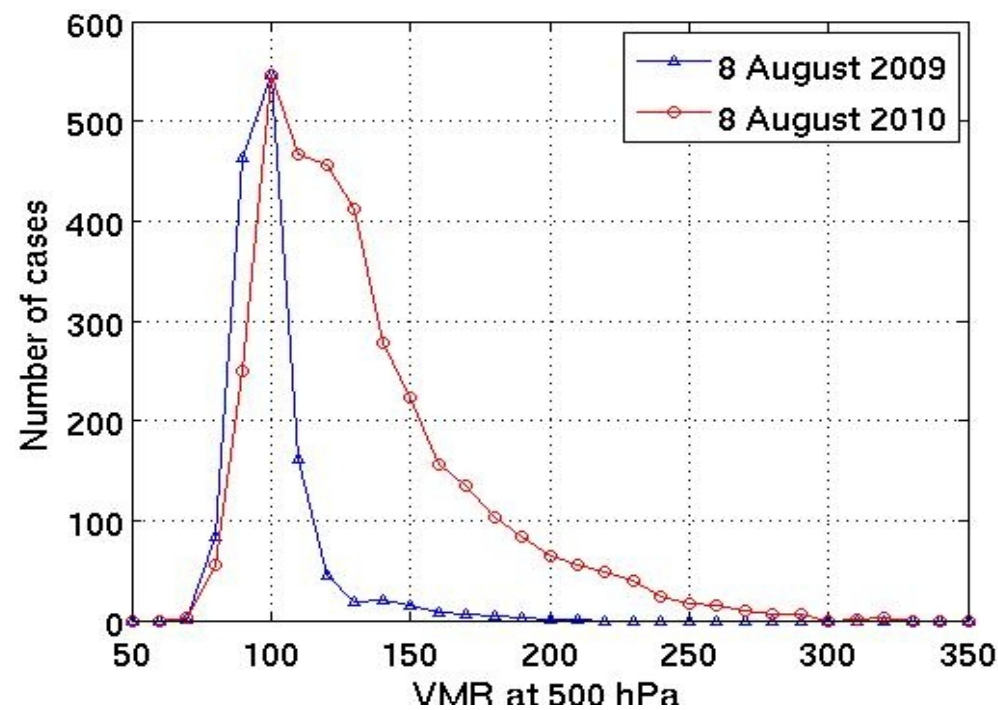


**Fig. 10.** Histograms of CO VMR-500 retrieved by AIRS for Russia in 8 August (day 220) of 2009 and 2010. Two boundary values, 150 ppb and 170 ppb, are used to calculate the plume areas in 2010.



## Satellite- and ground-based CO total column observations

L. Yurganov et al.

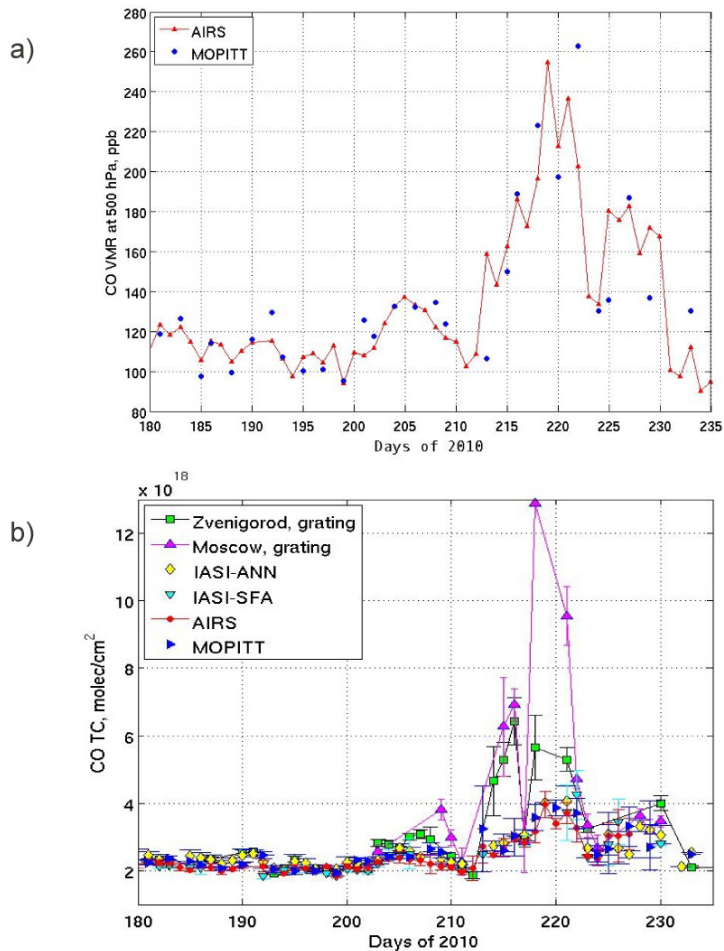


**Fig. 11.** VMR for 500 hPa (a) and CO TC (b) averaged over the Moscow environs (54.0°–58.0° N, 36.0°–38.0° E) in comparison to ground-based daily data.

[Title Page](#)
[Abstract](#)
[Introduction](#)
[Conclusions](#)
[References](#)
[Tables](#)
[Figures](#)
[◀](#)
[▶](#)
[◀](#)
[▶](#)
[Back](#)
[Close](#)
[Full Screen / Esc](#)
[Printer-friendly Version](#)
[Interactive Discussion](#)

## Satellite- and ground-based CO total column observations

L. Yurganov et al.

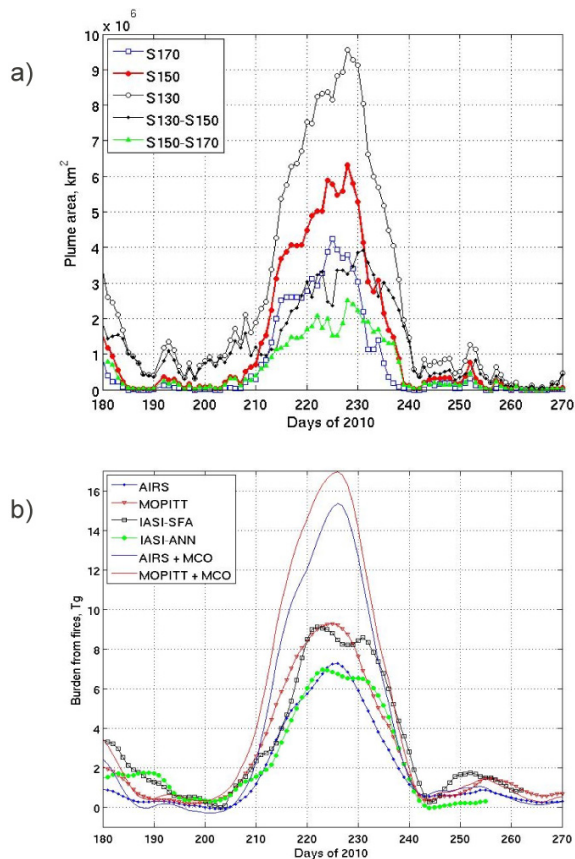


**Fig. 12.** (a) Plume area  $S$  for 3 selected boundaries (170, 150, and 130 ppb) over Russia in 2010. The differences  $S_{130}-S_{150}$  and  $S_{150}-S_{170}$  are plotted as well. (b) CO extra burden due to fires (total burden subtracted by background). First four lines are for standard retrieval. Last two lines demonstrate the effect of correction for MCO in the case of 150 ppb as a boundary of the plume.

## Satellite- and ground-based CO total column observations

L. Yurganov et al.

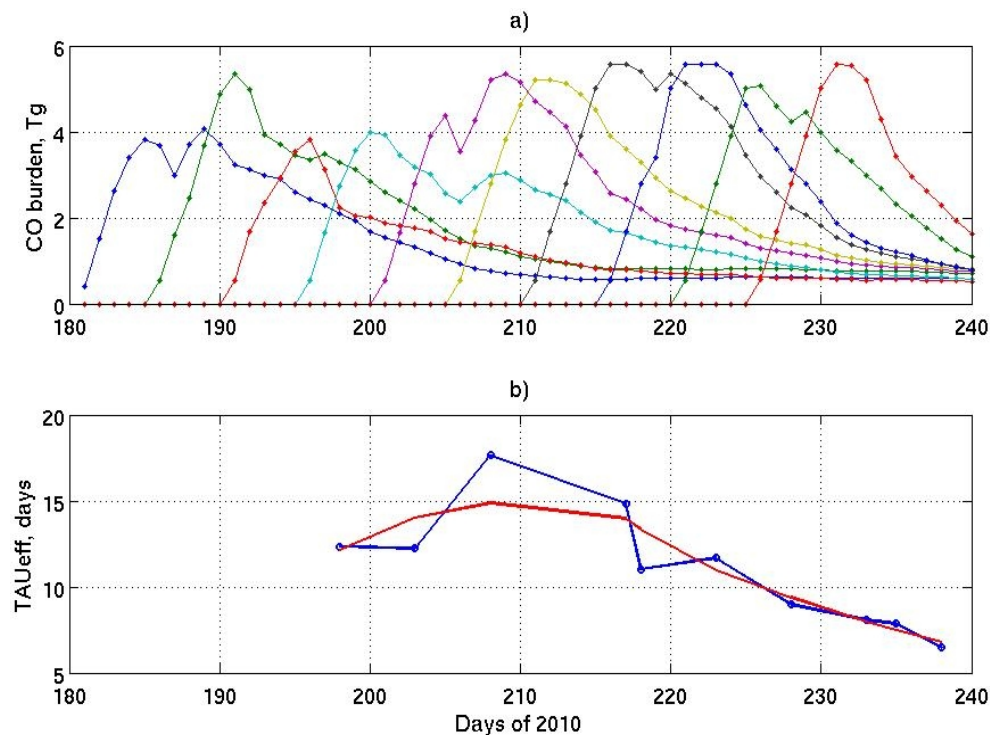


**Fig. 13.** (a) Simulated pyrogenic CO burden  $B$  over Russia in 2010 for 5-days-long idealized fires emitted  $1.11 \text{ Tg day}^{-1}$  for 10 cases; 1st case is for 1–5 July (days 182–186), 2nd for 6–10 July (days 187–191), etc. (b) Effective time parameter  $\text{TAU}_{\text{trans}}$  for the exponential decay of CO burden after the termination of simulated fire. Each point is averaged over periods of 12–16 days long. The red line is a smoothing approximation.

[Title Page](#)
[Abstract](#)
[Introduction](#)
[Conclusions](#)
[References](#)
[Tables](#)
[Figures](#)
[⏪](#)
[⏩](#)
[◀](#)
[▶](#)
[Back](#)
[Close](#)
[Full Screen / Esc](#)
[Printer-friendly Version](#)
[Interactive Discussion](#)

## Satellite- and ground-based CO total column observations

L. Yurganov et al.

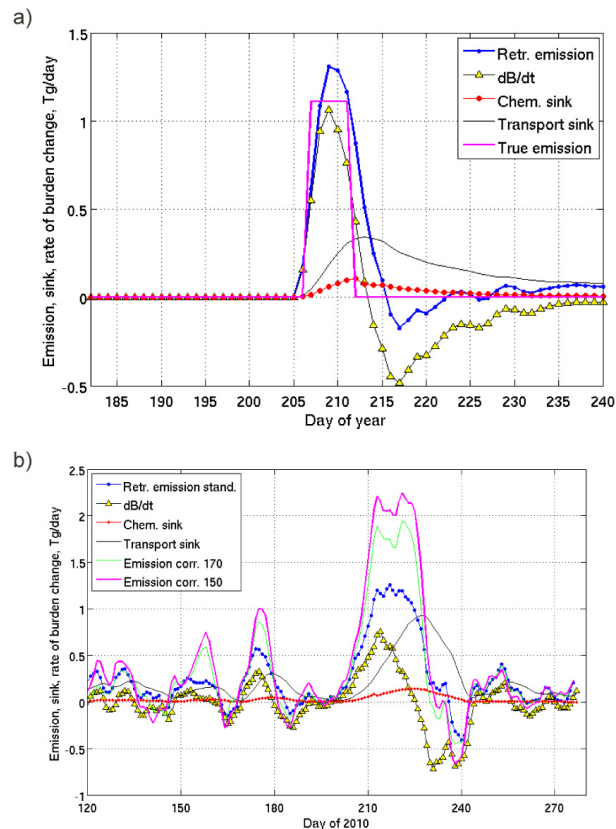


**Fig. 14.** (a) A test of the mass balance model. Magenta line is the emission of simulated fire (“true emission”) in the central Russia with  $1.11 \text{ Tg day}^{-1}$  ( $5.55 \text{ Tg}$  of total emission). For CO burden calculated by the GEOS-5 see Fig. 13a.  $[\text{OH}]$  for the chemical sink is according to Spivakovsky et al. (2000). The transport sink is calculated as  $B / \tau_{\text{trans}}$  (see Fig. 13). The retrieved emission rate is plotted as the blue line and dots. Retrieved total emitted CO for this case is  $7.67 \text{ Tg}$  that is 38% larger than set in the model. (b) The CO fire emission retrieved from MOPITT V4 data. The blue line with dots is for measured burdens. Measured burdens were added by MCO, and corrected emissions are plotted for two assumptions on the plume boundary:  $\text{VMR-500} > 150 \text{ ppb}$  and  $\text{VMR-500} > 170 \text{ ppb}$ .